

LA-UR-19-20376

Approved for public release; distribution is unlimited.

Title: A higher-order Lagrangian discontinuous Galerkin hydrodynamic method for solid dynamics and reactive materials

Author(s): Lieberman, Evan
Liu, Xiaodong
Morgan, Nathaniel Ray
Luscher, Darby Jon
Burton, Donald E.

Intended for: Report

Issued: 2019-01-18

Disclaimer:

Los Alamos National Laboratory, an affirmative action/equal opportunity employer, is operated by Triad National Security, LLC for the National Nuclear Security Administration of U.S. Department of Energy under contract 89233218CNA000001. By approving this article, the publisher recognizes that the U.S. Government retains nonexclusive, royalty-free license to publish or reproduce the published form of this contribution, or to allow others to do so, for U.S. Government purposes. Los Alamos National Laboratory requests that the publisher identify this article as work performed under the auspices of the U.S. Department of Energy. Los Alamos National Laboratory strongly supports academic freedom and a researcher's right to publish; as an institution, however, the Laboratory does not endorse the viewpoint of a publication or guarantee its technical correctness.

A higher-order Lagrangian discontinuous Galerkin hydrodynamic method for solid dynamics and reactive materials

Evan Lieberman

Co-Authors:

**Nathaniel Morgan (PI), Don Burton (co-PI),
Xiaodong Liu, D.J. Luscher**

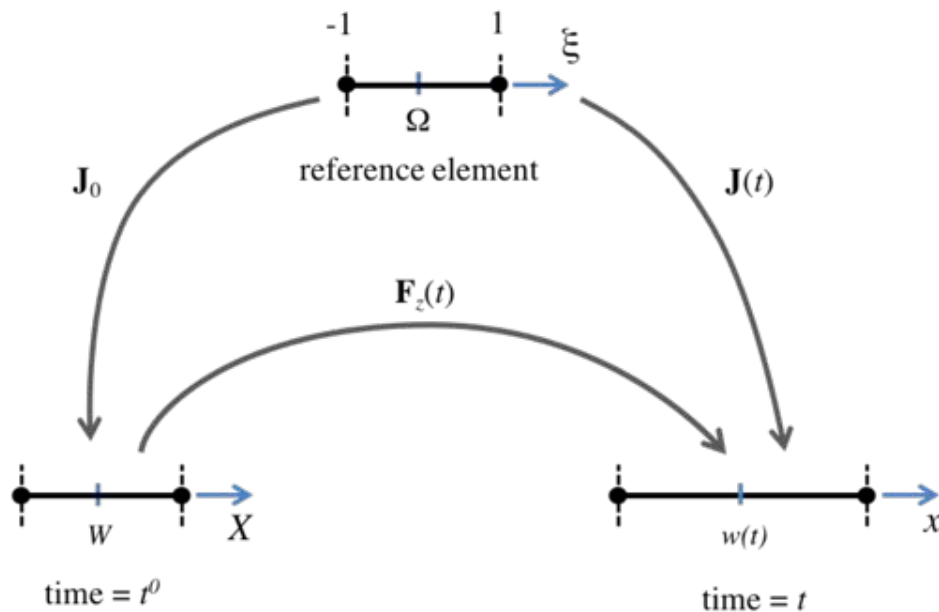
Acknowledgements:

**Konstantin Lipnikov,
Svetlana Tokareva, Mike Berry**



January 22, 2019
X: Computational Physics
Los Alamos National Laboratory

Lagrangian DG 1D Element and Quadratic Polynomial Details



$$\mathbb{U}(\xi, t) = \psi_1 \bar{\mathbb{U}}_z + \psi_2 \left. \frac{\partial \mathbb{U}}{\partial \xi} \right|_z + \psi_3 \left. \frac{\partial^2 \mathbb{U}}{\partial \xi^2} \right|_z$$

$$\psi_1 = 1$$

$$\psi_2 = \xi - \xi_z$$

$$\psi_3 = \frac{(\xi - \xi_z)^2}{2} - \frac{1}{\Omega} \int_{\Omega} \frac{(\xi - \xi_z)^2}{2} j^0 d\Omega$$

Summary of Lagrangian DG CCH equations for reference element

Basis functions: $\psi^l(\xi)$

Velocity: $\frac{d\mathbf{x}_p}{dt} = \mathbf{u}_p^*$

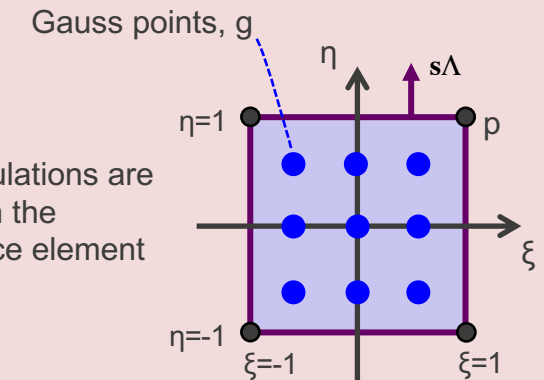
Mass matrix: $\mathbf{M}^{kl} = \sum_{g \in \Omega} \rho_g \psi_g^k \psi_g^l j_g \Omega_g$

Momentum: $\mathbf{M}^{kl} \frac{d\mathbf{u}^l}{dt} = \sum_{g \in \partial\Omega} \mathbf{s}_g \cdot (\psi_g^k j_g \mathbf{J}_g^{-1} \cdot \boldsymbol{\sigma}_g^*) \Lambda_g - \sum_{g \in \Omega} (\nabla_\xi \psi_g^k) \cdot (j_g \mathbf{J}_g^{-1} \cdot \boldsymbol{\sigma}_g) \Omega_g$

Total Energy: $\mathbf{M}^{kl} \frac{d\tau^l}{dt} = \sum_{g \in \partial\Omega} \mathbf{s}_g \cdot (\psi_g^k j_g \mathbf{J}_g^{-1} \cdot \boldsymbol{\sigma}_g^* \cdot \mathbf{u}_g^*) \Lambda_g - \sum_{g \in \Omega} (\nabla_\xi \psi_g^k) \cdot (j_g \mathbf{J}_g^{-1} \cdot \boldsymbol{\sigma}_g \cdot \mathbf{u}_g) \Omega_g$

Specific Volume: $\mathbf{M}^{kl} \frac{dv^l}{dt} = \sum_{g \in \partial\Omega} \mathbf{s}_g \cdot (\psi_g^k j_g \mathbf{J}_g^{-1} \cdot \mathbf{u}_g^*) \Lambda_g - \sum_{g \in \Omega} (\nabla_\xi \psi_g^k) \cdot (j_g \mathbf{J}_g^{-1} \cdot \mathbf{u}_g) \Omega_g$

Jacobi transformation: $\mathbf{J} = \nabla_\xi \Phi = \frac{\partial \mathbf{x}}{\partial \xi}$ $\Phi(\xi, t) = \sum_p \mathbf{x}_p \theta_p(\xi)$ $j = \det(\mathbf{J})$



Limiting of Modal Fields in High Order Lagrangian DG is Needed for Shocks

Barth-Jespersen Limiter

$$\phi = \begin{cases} \min \left(1, \frac{\alpha(\bar{U}^{max} - \bar{U})}{U(\xi_j) - \bar{U}} \right) & if \quad U(\xi_j) > 0 \\ \min \left(1, \frac{\alpha(\bar{U}^{min} - \bar{U})}{U(\xi_j) - \bar{U}} \right) & if \quad U(\xi_j) < 0 \\ 1 & else \end{cases}$$

Nodal Fields – Single Limiter

$$U(\xi_j)^{lim} = \bar{U} + \phi (U(\xi_j) - \bar{U})$$

Modal Fields – Hierarchical Limiting

$$U(\xi)^{lim} = \bar{U} + \phi_1 \left(\psi^2 \frac{\partial U}{\partial \xi} + \phi_2 \psi^3 \frac{\partial^2 U}{\partial \xi^2} \Big|_z \right)$$

D. Kuzmin. Slope limiting for discontinuous Galerkin approximations with a possibly non-orthogonal Taylor basis. *International Journal for Numerical Methods in Fluids*, 2013.

Outline

- **Solid Mechanics Models**
 - Deformation Mechanics
 - Constitutive Models
 - Analytic 1D Test Problem
 - 2D Test Problems
 - Summary
- **Reactive Models**
 - ZND Detonation Wave
 - Models
 - Results
 - Summary

Outline

- **Solid Mechanics Models**
 - Deformation Mechanics
 - Constitutive Models
 - Analytic 1D Test Problem
 - 2D Test Problems
 - Summary
- **Reactive Models**
 - ZND Detonation Wave
 - Models
 - Results
 - Summary

Overview of Deformation Mechanics

Velocity Gradient (\mathbf{L})

$$\mathbf{L} = \nabla_x \mathbf{u}$$

$$\mathbf{L} = \dot{\mathbf{F}} \mathbf{F}^{-1}$$

Deformation Gradient (\mathbf{F})

$$\mathbf{F} = \nabla_X \mathbf{x} = \frac{\partial \mathbf{x}}{\partial X}$$

$$\dot{\mathbf{F}} = \nabla_X \mathbf{u}$$

Strain Definitions

Infinitesimal: $\boldsymbol{\varepsilon} = \text{sym}(\nabla_X \mathbf{l})$

Right-Cauchy: $\mathbf{C} = \mathbf{F}^T \mathbf{F}$

Strain Rate ($\dot{\boldsymbol{\varepsilon}}$)

$$\dot{\boldsymbol{\varepsilon}} = \text{sym}(\mathbf{L})$$

Displacement Gradient ($\nabla_X \mathbf{l}$)

$$\nabla_X \mathbf{l} = \mathbf{F} - \mathbf{I}$$

Green-Lagrange: $\mathbf{E} = \frac{1}{2} (\mathbf{C} - \mathbf{I})$

Hydrostatic and Deviatoric

$$\boldsymbol{\sigma} = \boldsymbol{\sigma}' - p \mathbf{I}$$

$$\boldsymbol{\varepsilon}' = \boldsymbol{\varepsilon} - \text{Tr}(\boldsymbol{\varepsilon})/3$$

$$\mathbf{F}' = \det(\mathbf{F})^{-\frac{1}{3}} \mathbf{F}$$

Elastic and Plastic Components

$$\boldsymbol{\varepsilon} = \boldsymbol{\varepsilon}_e + \boldsymbol{\varepsilon}_p$$

$$\mathbf{F} = \mathbf{F}_e \mathbf{F}_p$$

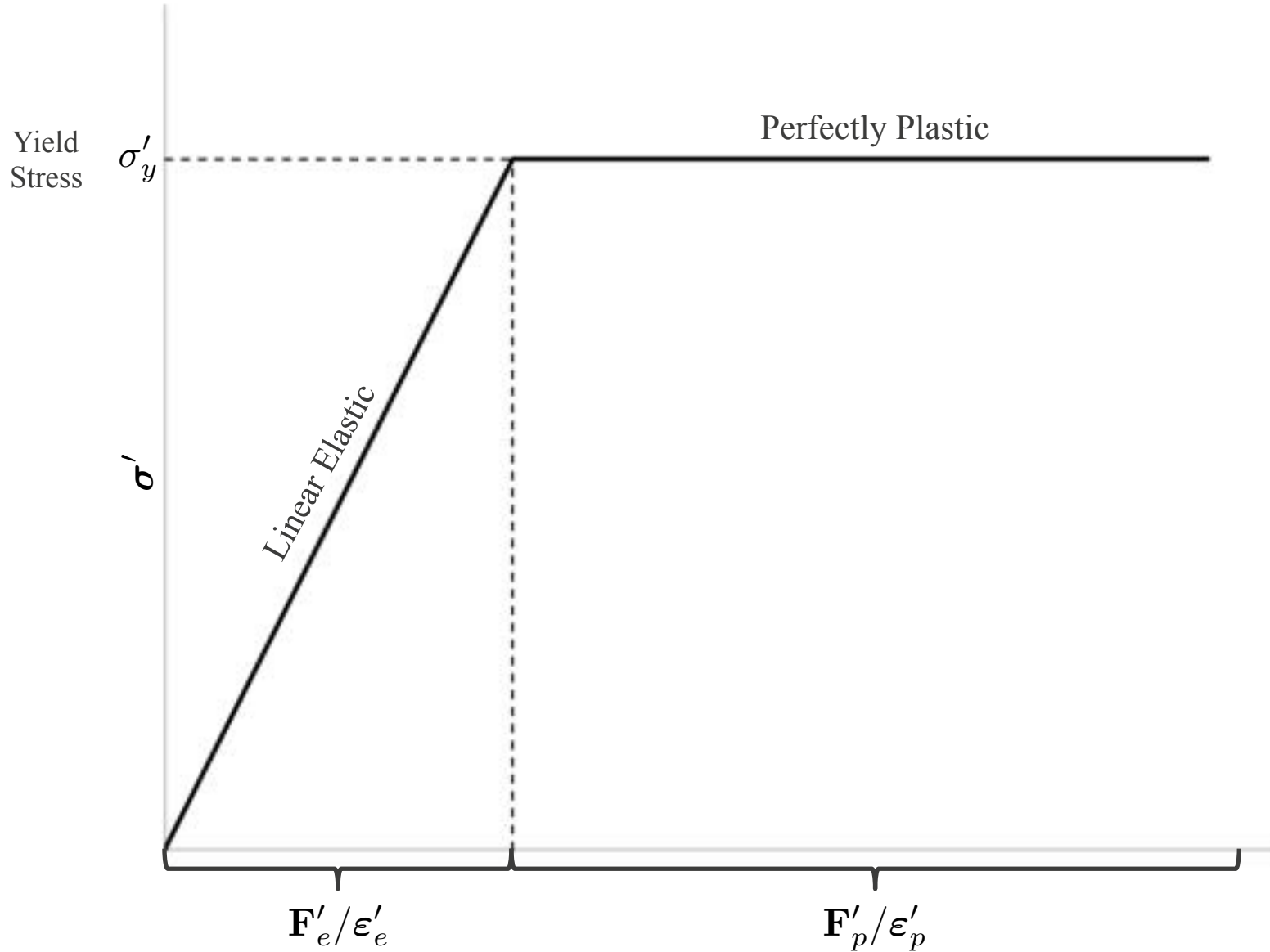
Lagrangian DG Equations for Velocity and Deformation Gradient

Volume matrix: $V_{qk} = \int_{\Omega(t)} \psi_q \psi_k j(t) d\Omega$

Velocity Gradient: $V_{qk} \cdot \mathbf{L}_k = \oint_{\partial\Omega} \mathbf{s} \cdot (\psi_q j \mathbf{J}^{-1} \mathbf{u}^*) d\Lambda - \int_{\Omega} (\nabla_{\xi} \psi_q) \cdot (j \mathbf{J}^{-1} \mathbf{u}) d\Omega$

Deformation Gradient:
Gradient: $V_{qk}^0 \cdot \frac{d\mathbf{F}_k}{dt} = \oint_{\partial\Omega} \mathbf{s} \cdot \left(\psi_q j^0 (\mathbf{J}^0)^{-1} \mathbf{u}^* \right) d\Lambda - \int_{\Omega} (\nabla_{\xi} \psi_q) \cdot \left(j^0 (\mathbf{J}^0)^{-1} \mathbf{u} \right) d\Omega$

Linear Elastic-Perfectly Plastic Behavior



Outline

- **Solid Mechanics Models**
 - Deformation Mechanics
 - Constitutive Models
 - Analytic 1D Test Problem
 - 2D Test Problems
 - Summary
- **Reactive Models**
 - ZND Detonation Wave
 - Models
 - Results
 - Summary

The Hypoelastic-Plastic Constitutive Model

Jaumann Stress Rate

$$\dot{\sigma}' = 2G(\dot{\varepsilon}' - \dot{\varepsilon}'_p) - \sigma' \dot{\omega} + \dot{\omega} \sigma'$$

$$\dot{\omega} = \text{asym}(\mathbf{L})$$

Trial Stress Rate:

- No rotation in 1D
- Assume no plastic flow

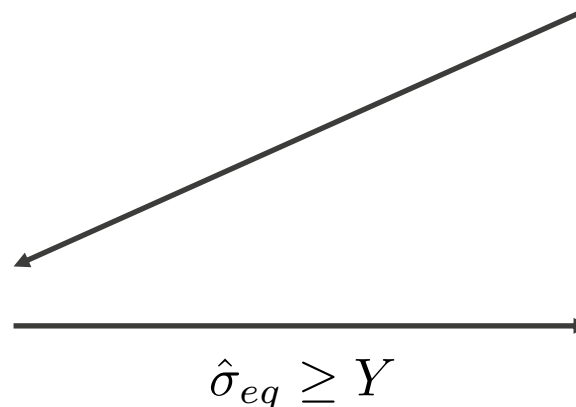
RK Time Integration:

$$\hat{\sigma}' = \sigma'^s + \Delta t \hat{\sigma}'$$

Radial Return

$$\sigma'^{s+1} = \hat{\sigma}' \frac{Y}{\hat{\sigma}_{eq}}$$

$$\hat{\sigma}_{eq} = \sqrt{\frac{3}{2} \hat{\sigma}' : \hat{\sigma}'}$$



The Infinitesimal Hyperelastic-Plastic Constitutive Model

Linear Elasticity

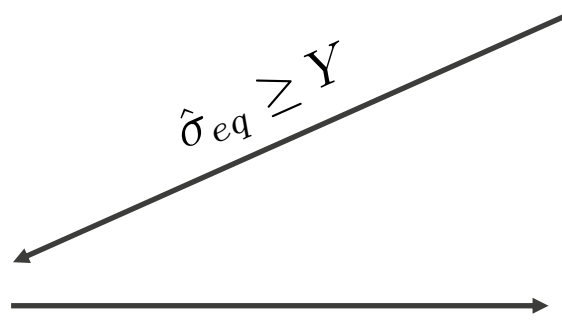
$$\sigma' = 2G(\epsilon' - \epsilon'_p)$$

Trial Stress:
 - Assume no new plastic strain
 $\hat{\sigma}' = 2G(\epsilon'^{s+1} - \epsilon_p^s)$

Radial Return

$$\sigma'^{s+1} = \hat{\sigma}' \frac{Y}{\hat{\sigma}_{eq}}$$

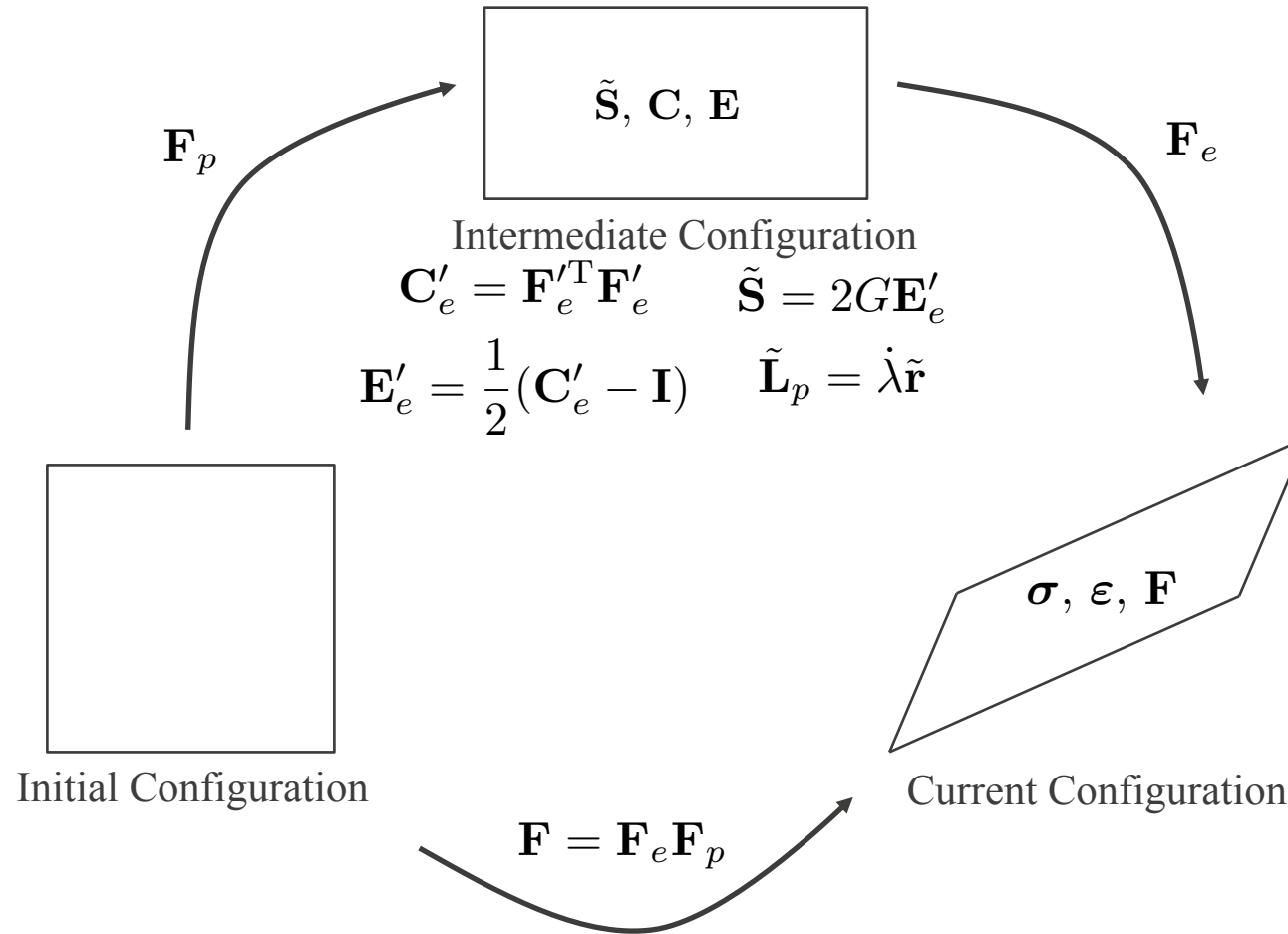
$$\hat{\sigma}_{eq} = \sqrt{\frac{3}{2} \hat{\sigma}' : \hat{\sigma}'}$$



Update Plastic Strain

$$\epsilon_p^{s+1} = \epsilon'^{s+1} - (2G)^{-1} \sigma'^{s+1}$$

The Finite Hyperelastic-Plastic Constitutive Model



Outline

- **Solid Mechanics Models**
 - Deformation Mechanics
 - Constitutive Models
 - Analytic 1D Test Problem
 - 2D Test Problems
 - Summary
- **Reactive Models**
 - ZND Detonation Wave
 - Models
 - Results
 - Summary

New Hyperelastic Analytic Solutions for a 1D Elastic-plastic Piston

Hypoelastic

$$\dot{\sigma}' = 2G\dot{\varepsilon}' = 2G \left(\frac{2}{3}L \right)$$

$$\sigma' = \frac{4}{3}G \int L dt$$

$$-\frac{Y}{2G} = \int_{t_0}^{t_y} L dt = \int_{t_0}^{t_y} \frac{\dot{V}}{V} dt$$

$$-\frac{Y}{2G} = \ln \left(\frac{V_y}{V_0} \right) = \ln \left(\frac{\rho_0}{\rho_y} \right)$$

$$\frac{\rho_0}{\rho_y} = \exp \left(-\frac{Y}{2G} \right)$$

$$\sigma'_y = -\frac{2}{3}Y$$

$$F_y = \frac{\rho_0}{\rho_y}$$

Infinitesimal Hyperelastic

$$\sigma' = 2Ge = 2G \left(\frac{2}{3}\varepsilon \right)$$

$$\varepsilon_y = -\frac{Y}{2G}$$

$$F_y - 1 = \frac{\rho_0}{\rho_y} - 1 = -\frac{Y}{2G}$$

$$\boxed{\frac{\rho_0}{\rho_y} = 1 - \frac{Y}{2G}}$$

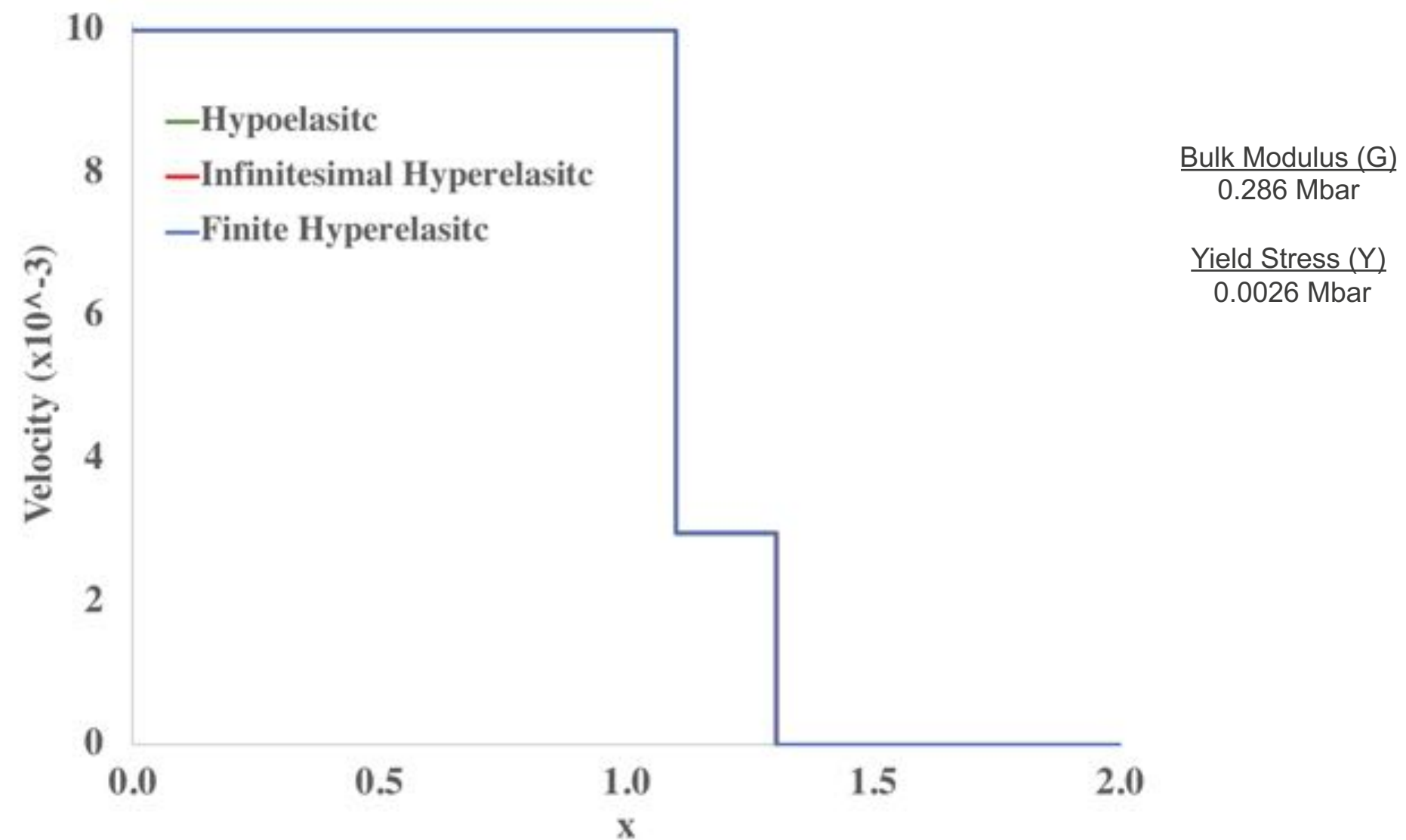
Finite Hyperelastic

$$F_y^{7/3} - F_y^{-5/3} + F_y^{-1} - F_y = -\frac{Y}{G}$$

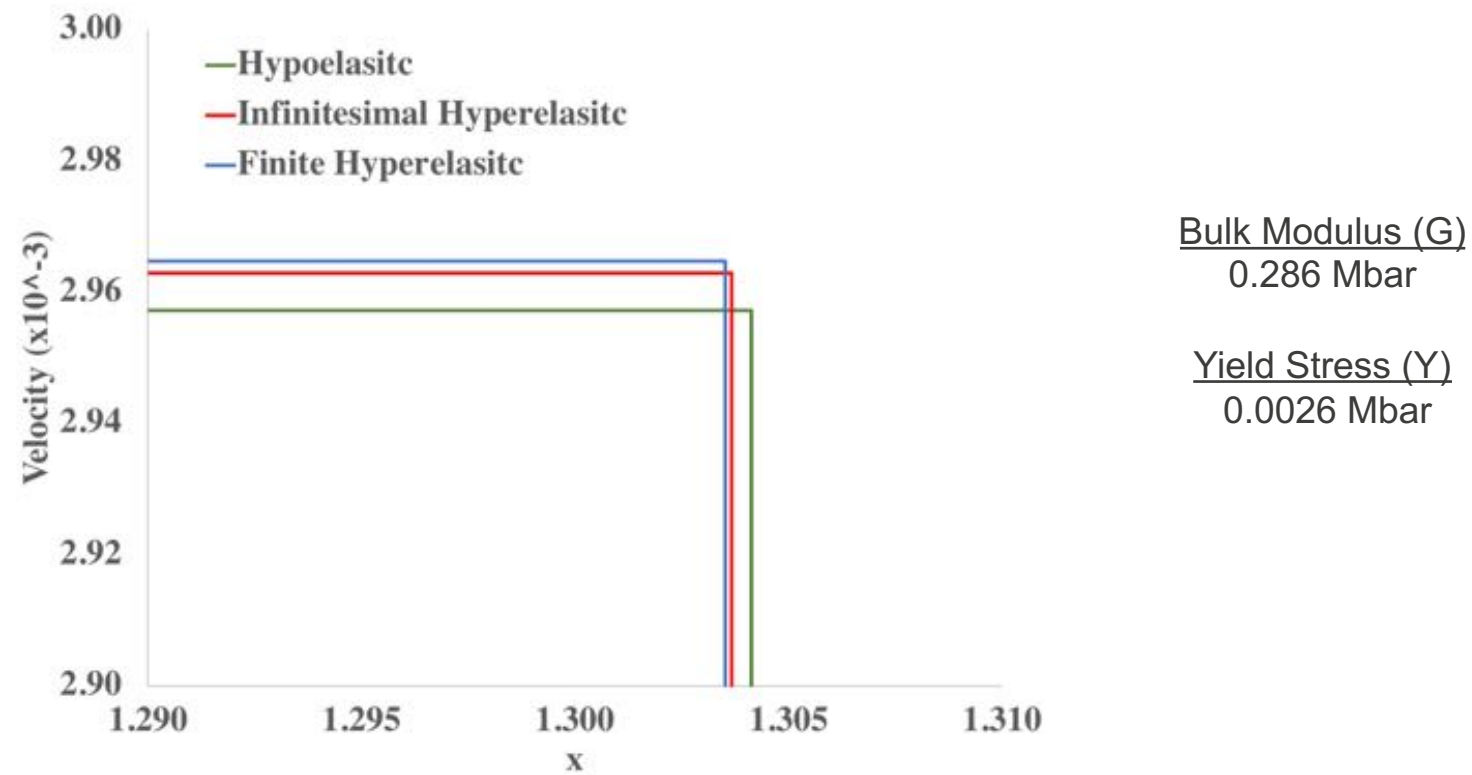
H.S. Udaykumar, L. Tran, D.M. Belk, and K.J. Vanden. An Eulerian method for computation of multimaterial impact with ENO shock-capturing and sharp interfaces. *Journal of Computational Physics*, 2003.

E.J. Lieberman, X. Liu, N.R. Morgan, D.J. Luscher, and D.E. Burton. A higher-order Lagrangian discontinuous Galerkin hydrodynamic method for solid dynamics. *Computer Methods in Applied Mechanics and Engineering*, In Review.

Analytic Solution to the 1D Elastic-plastic Piston for Different Models

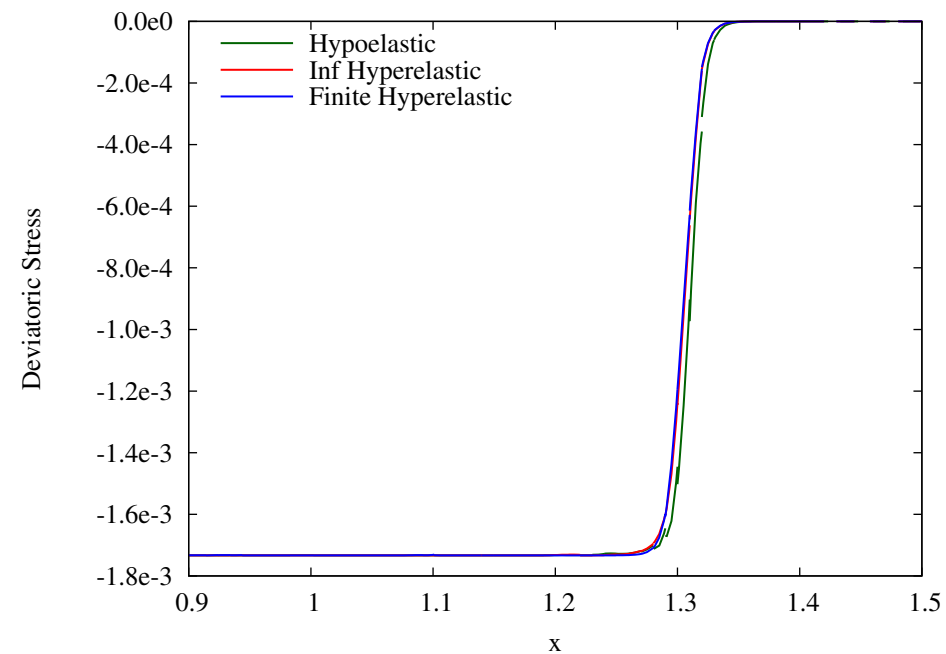
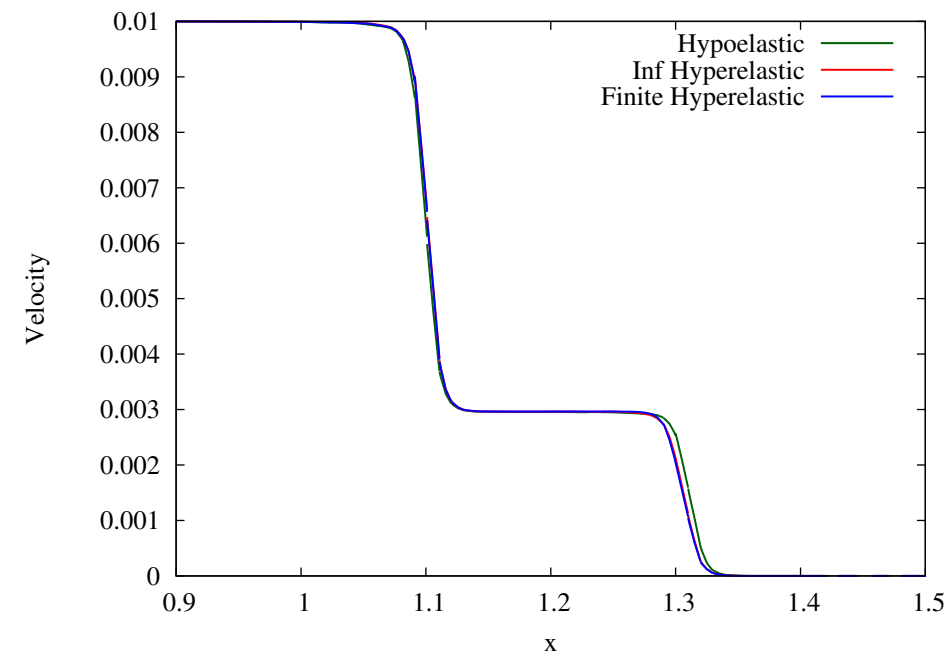


Analytic Solution to the 1D Elastic-plastic Piston is Different for Different Models

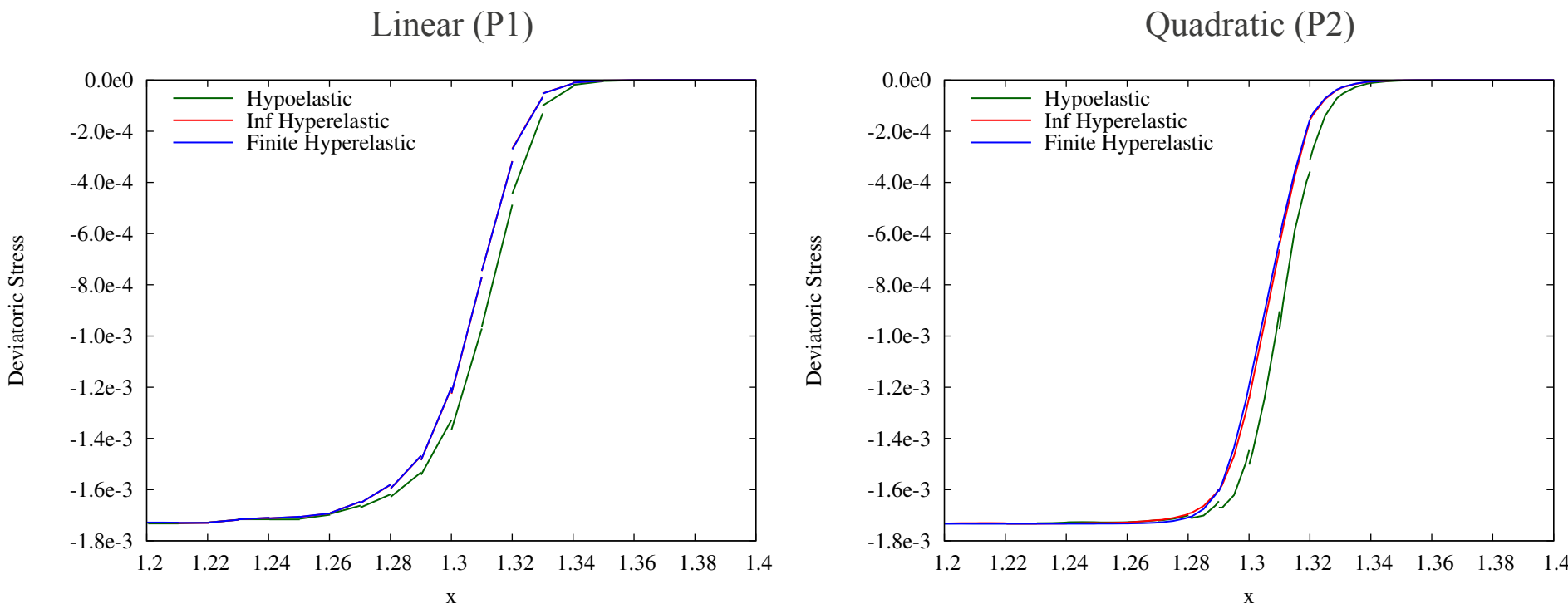


	Hypoelastic		Infinitesimal Hyperelastic		Finite Hyperelastic	
	Elastic Wave	Plastic Wave	Elastic Wave	Plastic Wave	Elastic Wave	Plastic Wave
Wave Speed (cm/ μ s)	0.652064	0.550531	0.651831	0.550542	0.651756	0.550545
Velocity (cm/ μ s)	2.9572e-03	0.01	2.9629e-03	0.01	2.9647e-03	0.01
Density (g/cm 3)	2.8027107	2.8392283	2.8027397	2.8392276	2.8027492	2.8392274
Pressure (Mbar)	3.6466e-03	1.4455e-02	3.6550e-03	1.4455e-02	3.6577e-03	1.4455e-02
Dev. Stress (Mbar)	-1.7333e-03	-1.7333e-03	-1.7333e-03	-1.7333e-03	-1.7333e-03	-1.7333e-03

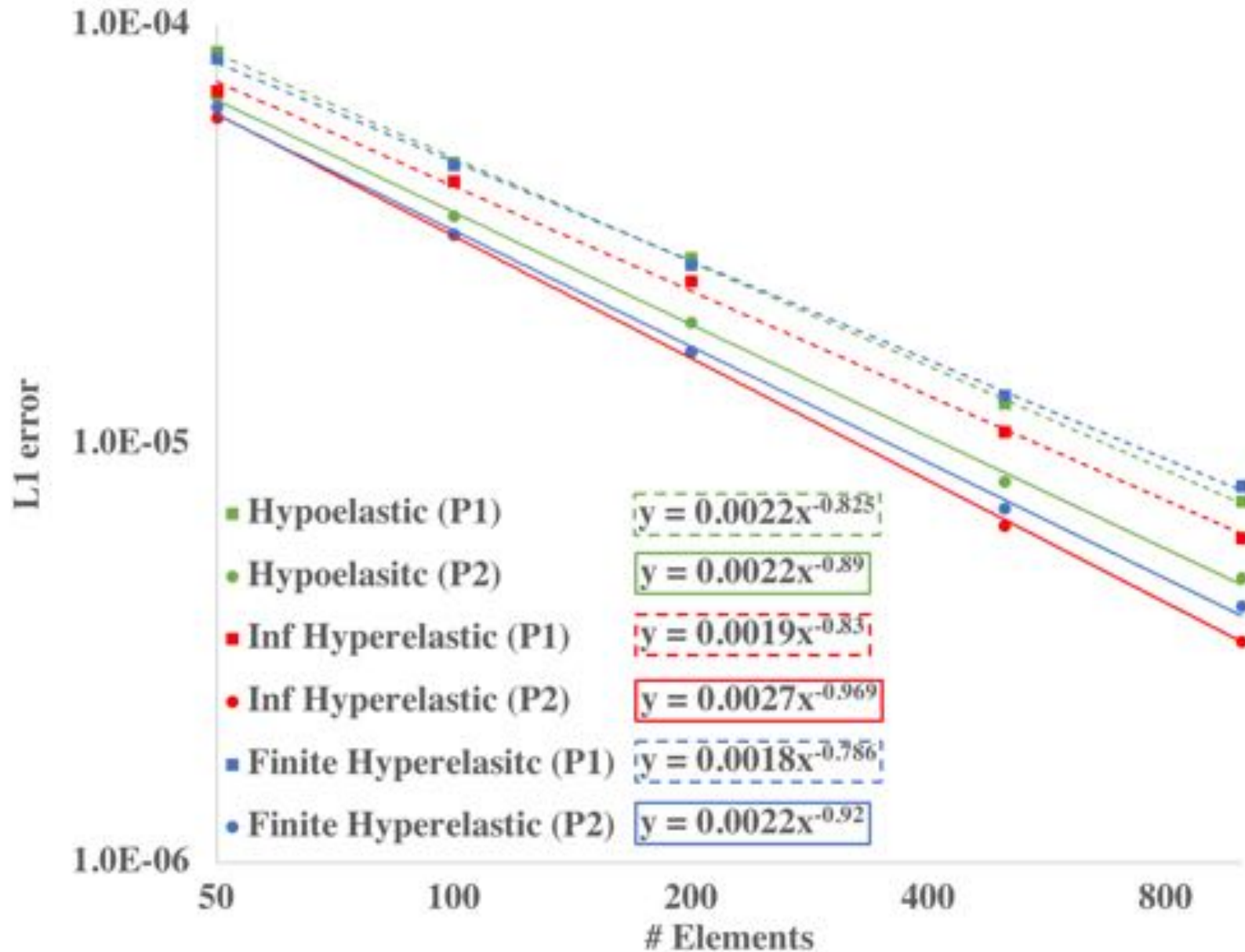
Results for the Elastic-plastic Piston for all Models with DG(P2)



DG(P2) Results have Sharper Shock Front and Smoother Results than DG(P1)



DG(P2) Shows Greater Accuracy and Faster Convergence than DG(P1)

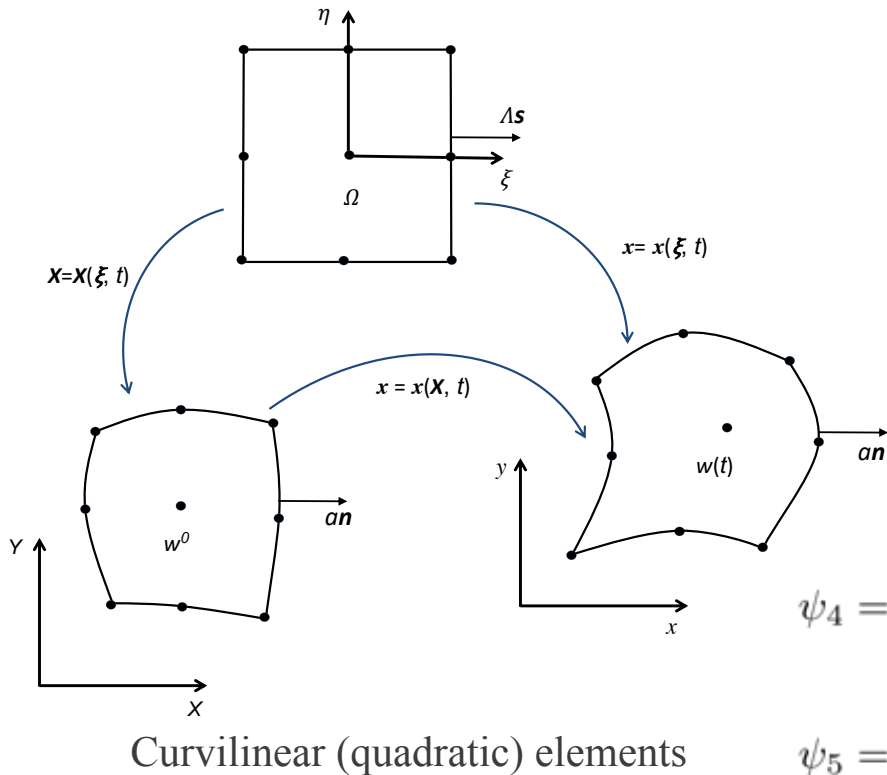


Outline

- **Solid Mechanics Models**
 - Deformation Mechanics
 - Constitutive Models
 - Analytic 1D Test Problem
 - 2D Test Problems
 - Summary
- **Reactive Models**
 - ZND Detonation Wave
 - Models
 - Results
 - Summary

Lagrangian DG 2D Element and Quadratic Polynomial Details

$$\mathbb{U}(\xi, \eta, t) = \psi_1 \bar{\mathbb{U}}_z + \psi_2 \frac{\partial \mathbb{U}_k}{\partial \xi} \Big|_z + \psi_3 \frac{\partial \mathbb{U}_k}{\partial \eta} \Big|_z + \psi_4 \frac{\partial^2 \mathbb{U}_k}{\partial \xi^2} \Big|_z + \psi_5 \frac{\partial^2 \mathbb{U}_k}{\partial \eta^2} \Big|_z + \psi_6 \frac{\partial^2 \mathbb{U}_k}{\partial \xi \partial \eta} \Big|_z$$



$$\psi_1 = 1$$

$$\psi_2 = \xi - \xi_{cm}$$

$$\psi_3 = \eta - \eta_{cm}$$

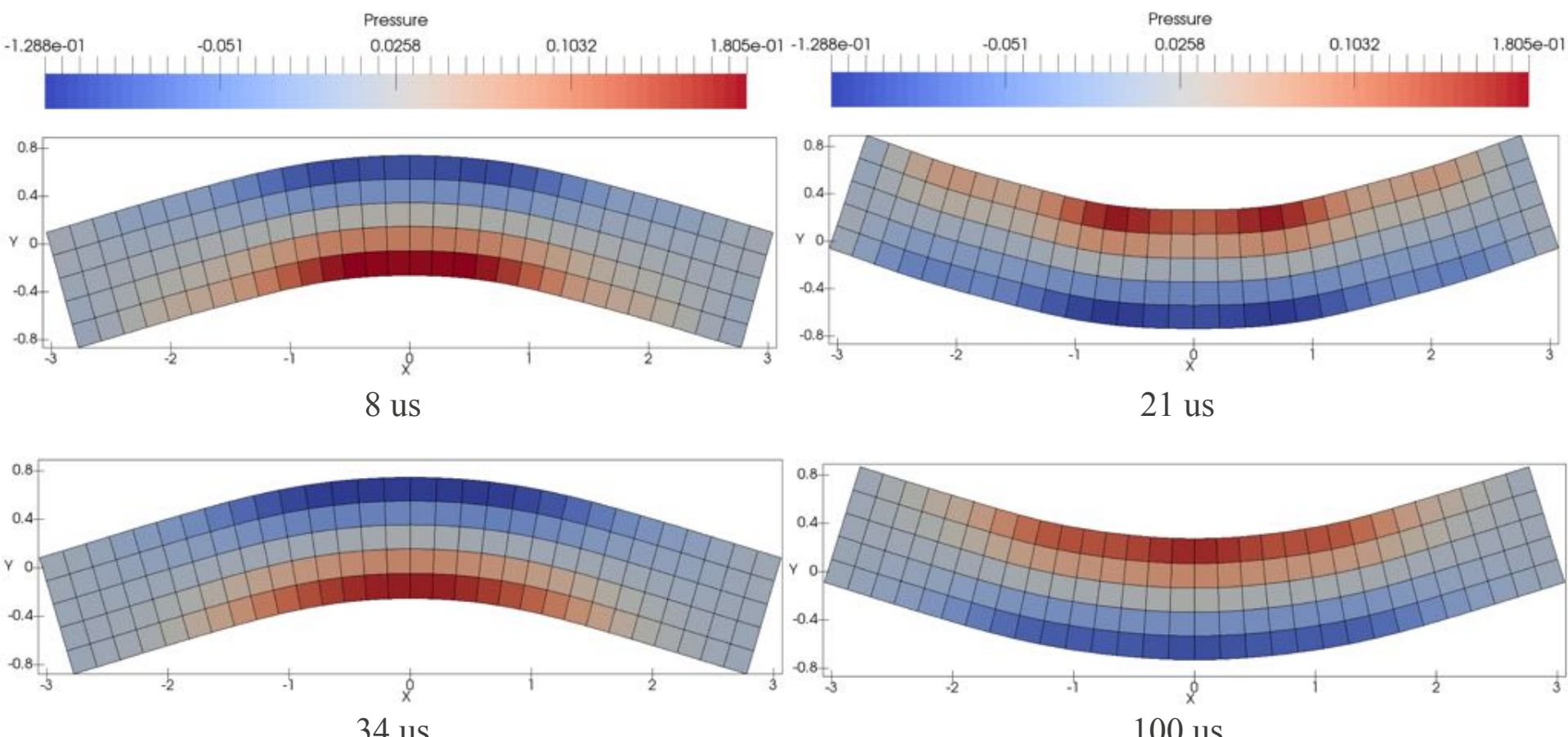
$$\psi_4 = \frac{(\xi - \xi_{cm})^2}{2} - \frac{1}{m} \int_{\Omega} \rho \frac{(\xi - \xi_{cm})^2}{2} j^0 d\Omega$$

$$\psi_5 = \frac{(\eta - \eta_{cm})^2}{2} - \frac{1}{m} \int_{\Omega} \rho \frac{(\eta - \eta_{cm})^2}{2} j^0 d\Omega$$

$$\psi_6 = (\xi - \xi_{cm})(\eta - \eta_{cm}) - \frac{1}{m} \int_{\Omega} \rho (\xi - \xi_{cm})(\eta - \eta_{cm}) j^0 d\Omega$$

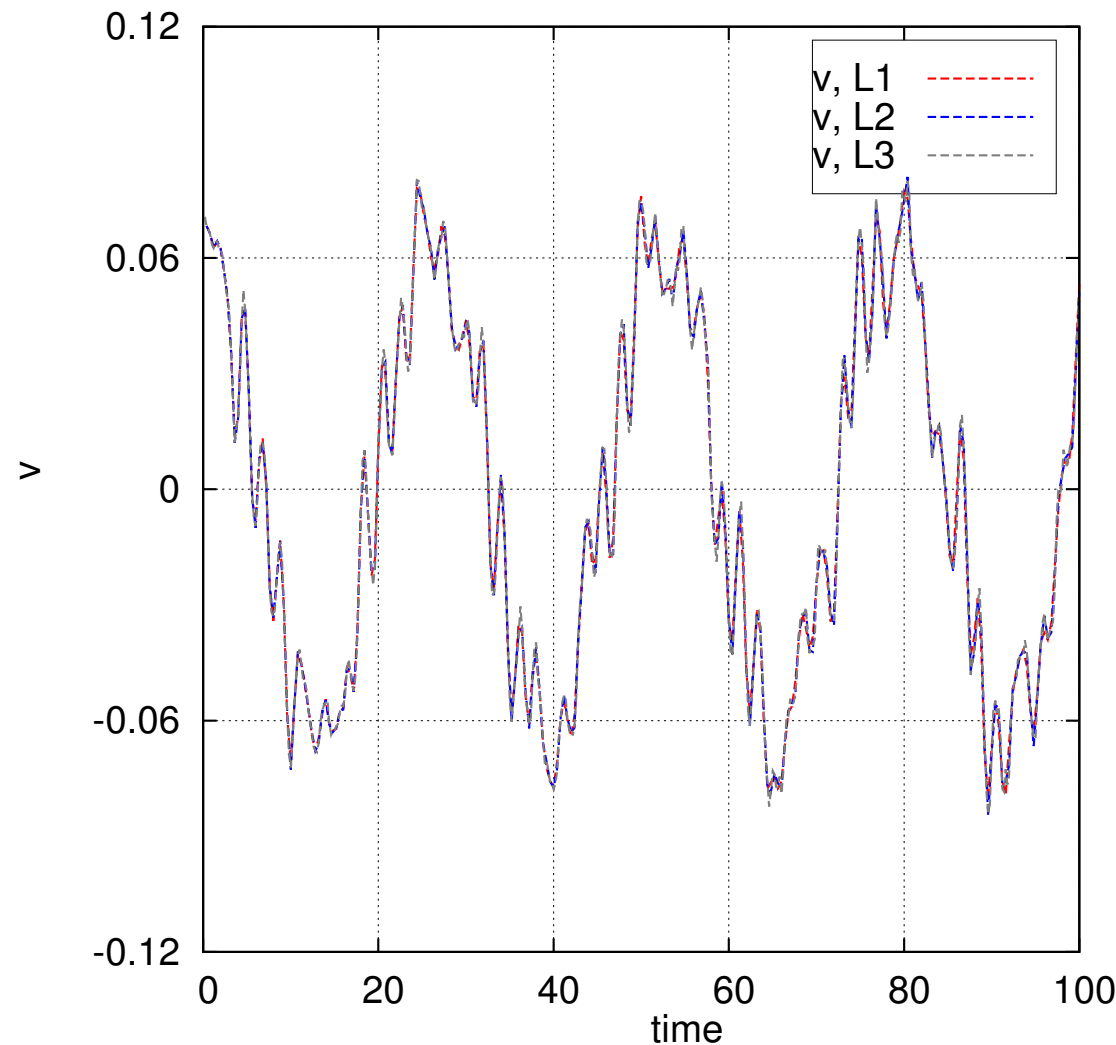
X. Liu, N.R. Morgan, and D.E. Burton. A high-order Lagrangian discontinuous galerkin hydrodynamic method for quadratic cells with a subcell mesh stabilization scheme. *Journal of Computational Physics*, In Revision.

Bending Beam Results Show Dissipation Errors are Exceptionally Small



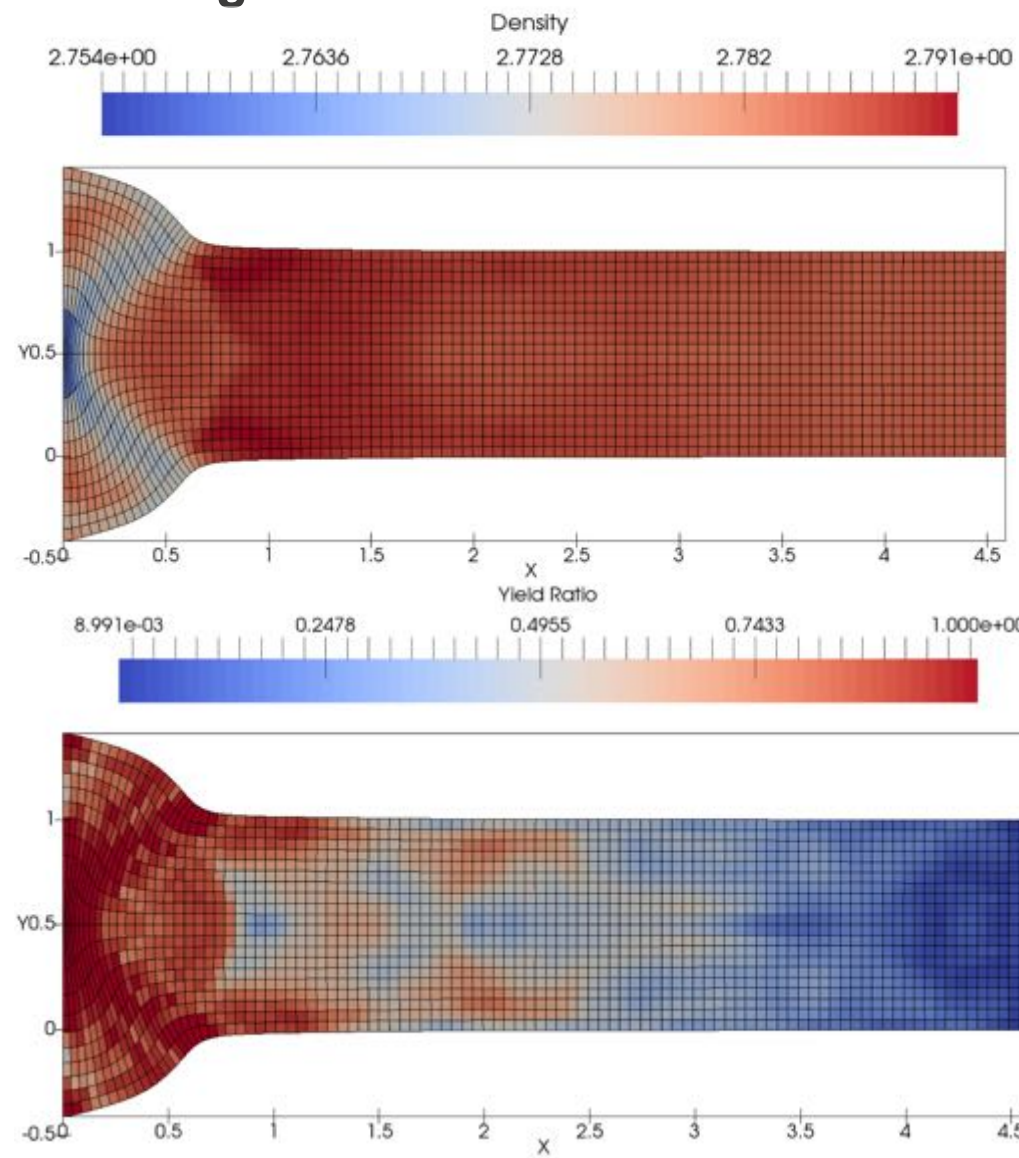
2D Finite Elastic

2D Finite Hyperelastic Bending Beam Does Not Dissipate Oscillating Velocity



Taylor Anvil Impact Results with DG(P2) and High Order Elements are Robust Under Large Plastic Deformations

2D Infinitesimal
Elastic-Plastic



Outline

- **Solid Mechanics Models**
 - Deformation Mechanics
 - Constitutive Models
 - Analytic 1D Test Problem
 - 2D Test Problems
 - Summary
- **Reactive Models**
 - ZND Detonation Wave
 - Models
 - Results
 - Summary

Solid Mechanics Summary

- The analytic solution to an elastic-plastic problem will change with the type of model used to represent the mechanical behavior.
- For modeling strength behavior in metals, piece-wise constant polynomials performed very poorly compared to linear and quadratic polynomials.
- Quadratic polynomials consistently resulted in more accurate solutions and faster overall convergence than linear polynomials.
- The infinitesimal hyperelastic-plastic model resulted in more accurate solutions and faster convergence than the other models.

Future Work for Solid Mechanics

- Allow non-constant materials parameters such as variable elastic moduli or plastic hardening.
- Add more advanced physical behavior such as anisotropy, crystal plasticity, and dilatational plasticity (damage).

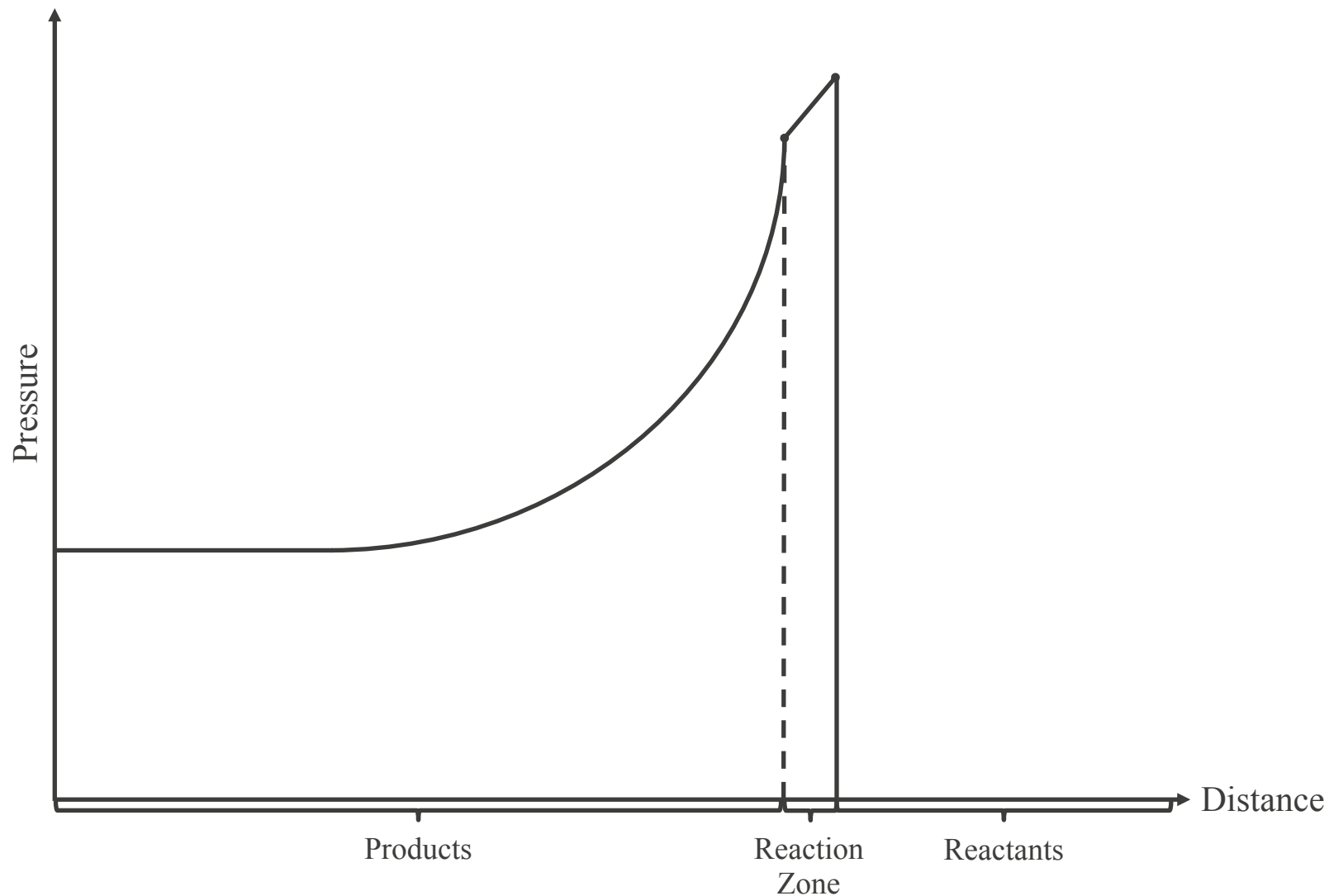
Outline

- **Solid Mechanics Models**
 - Deformation Mechanics
 - Constitutive Models
 - Analytic 1D Test Problem
 - 2D Test Problems
 - Summary
- **Reactive Models**
 - ZND Detonation Wave
 - Models
 - Results
 - Summary

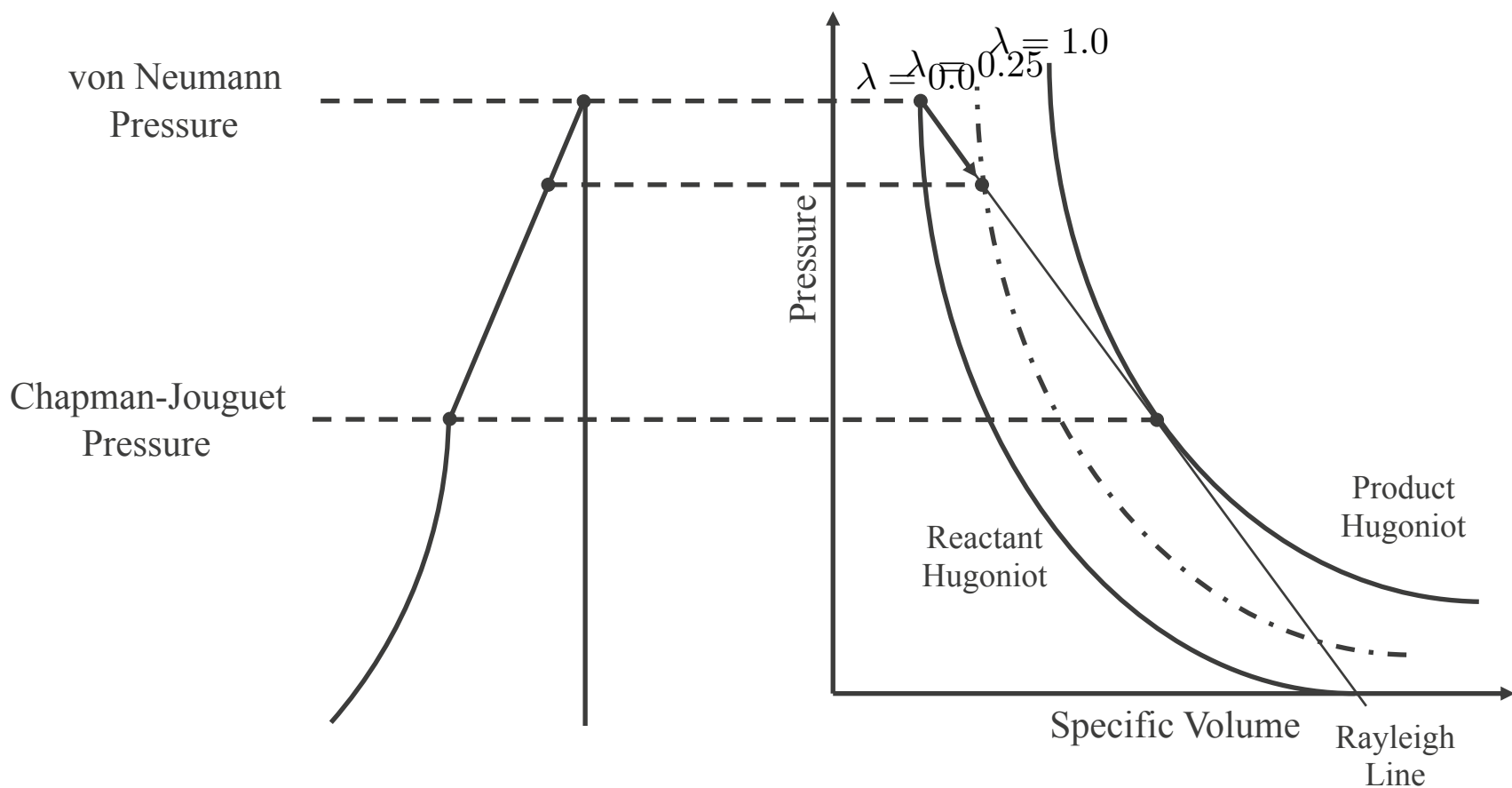
Outline

- **Solid Mechanics Models**
 - Deformation Mechanics
 - Constitutive Models
 - Analytic 1D Test Problem
 - 2D Test Problems
 - Summary
- **Reactive Models**
 - ZND Detonation Wave
 - Models
 - Results
 - Summary

Zeldovich-von Neumann-Döring (ZND) Detonation Wave Structure has Finite Reaction Rate



Zeldovich-von Neumann-Döring (ZND) Detonation Wave is Based on the Hugoniot



Outline

- **Solid Mechanics Models**
 - Deformation Mechanics
 - Constitutive Models
 - Analytic 1D Test Problem
 - 2D Test Problems
 - Summary
- **Reactive Models**
 - ZND Detonation Wave
 - Models
 - Results
 - Summary

Multiphase Model Uses Two Equations of State with Pressure-Temperature Equilibrium

Davis Equations of State

Known

$$\lambda, e(\xi), \nu(\xi)$$

Davis Reactant EOS

$$p_r(e_1, \nu_1) = p_r^s(\nu_1) + \frac{\Gamma_r(\nu_1)}{\nu_1} (e_1 - e_r^s(\nu_1))$$

$$T_r(e_1, \nu_1)$$

P-T Equilibrium

$$p_r(e_1(\xi), \nu_1(\xi)) = p_p(e_2(\xi), \nu_2(\xi))$$

$$T_r(e_1(\xi), \nu_1(\xi)) = T_p(e_2(\xi), \nu_2(\xi))$$

$$e(\xi) = (1 - \lambda(\xi))e_1(\xi) + \lambda(\xi)e_2(\xi)$$

$$\nu(\xi) = (1 - \lambda(\xi))\nu_1(\xi) + \lambda(\xi)\nu_2(\xi)$$

Davis Product EOS

Unknown

$$e_1, e_2, \nu_1, \nu_2$$

$$p_p(e_2, \nu_2) = p_p^s(\nu_2) + \frac{\Gamma_p(\nu_2)}{\nu_2} (e_2 - e_p^s(\nu_2) + e_{src})$$

$$T_p(e_2, \nu_2)$$

B.L. Wescott, D.S. Stewart, and W.C. Davis. Equation of state and reaction rate for condensed-phase explosives. *Journal of Applied Physics*, 2005.

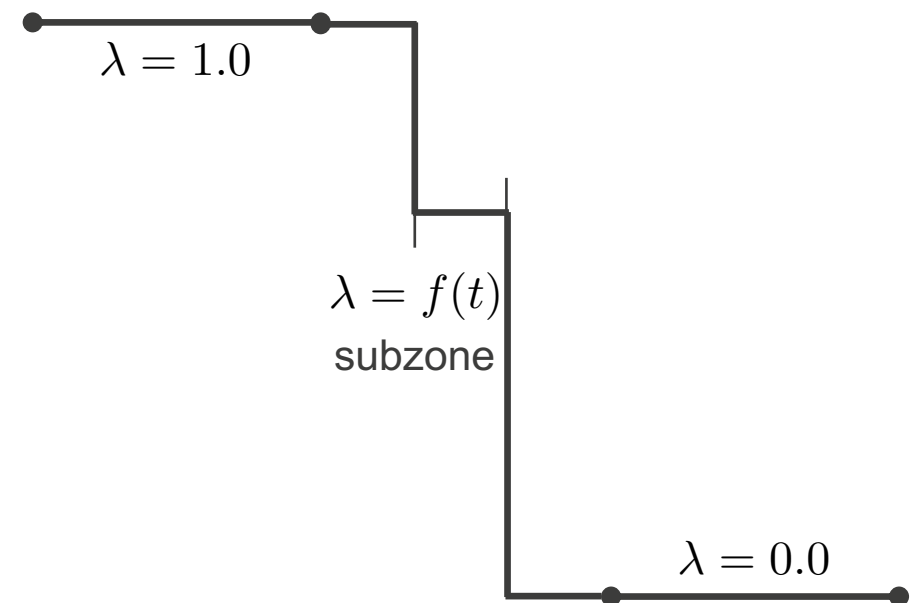
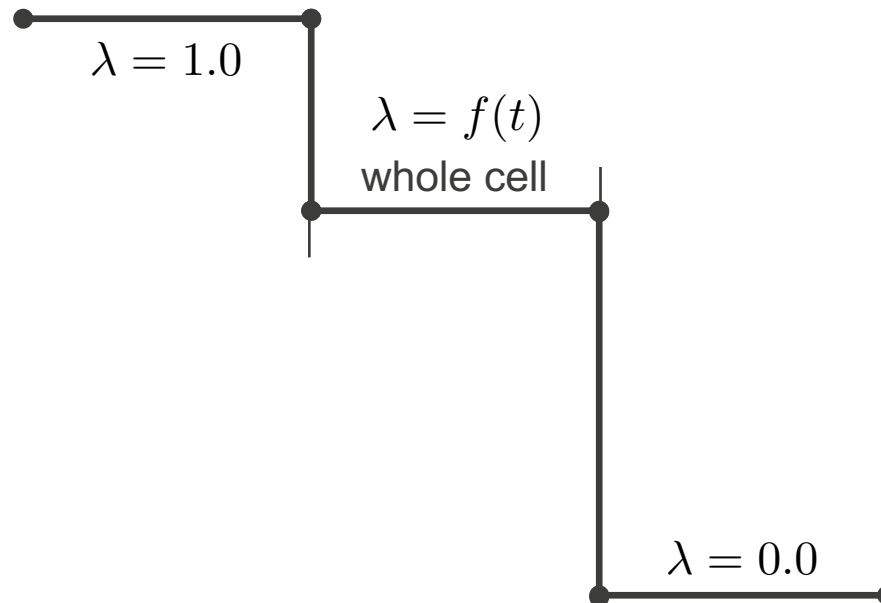
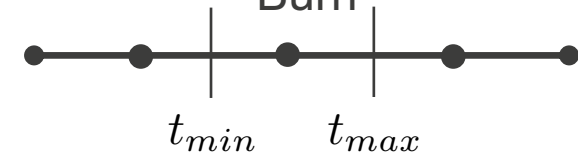
Programmed Burn Model in DG Is Improved Using Subzone Methods

$$\lambda = \frac{t - t_{min}}{t_{max} - t_{min}}$$

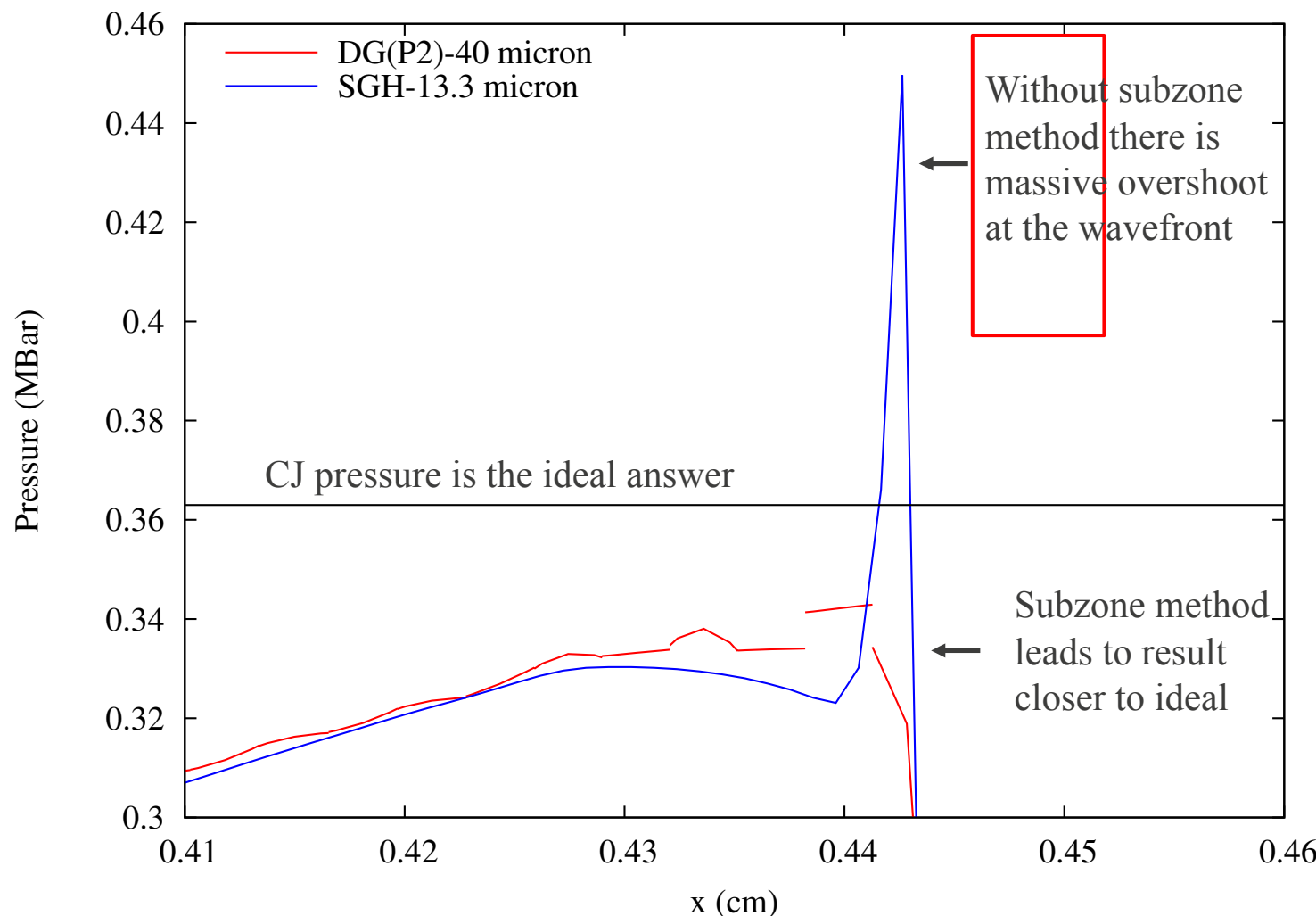
Programmed Burn



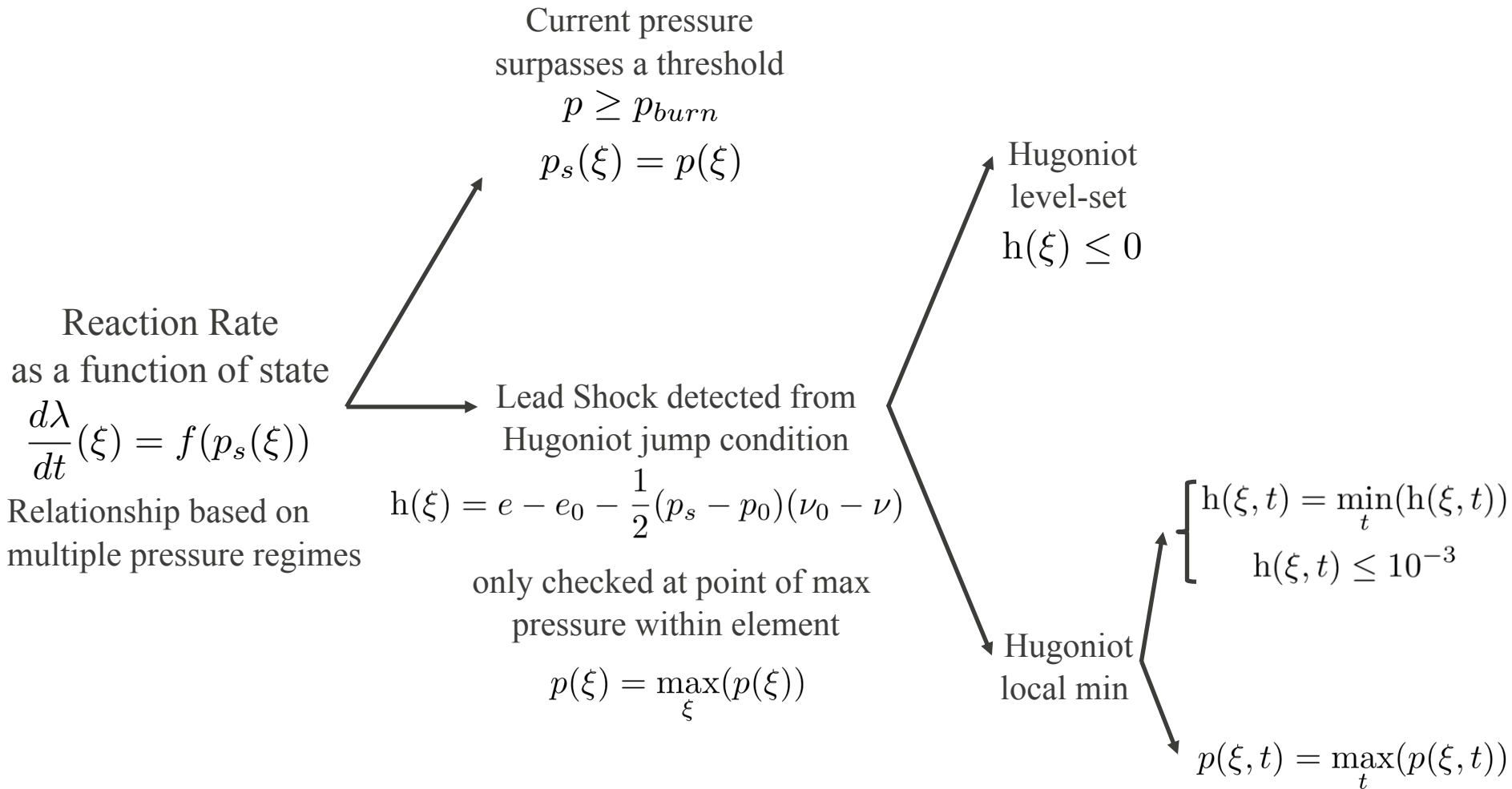
Subzone Programmed Burn



DG with Subzone Method Avoids Spurious Overshoots in Programmed Burn



Scaled Unified Reactive Front (SURF) Model is a Function of Lead Shock Pressure

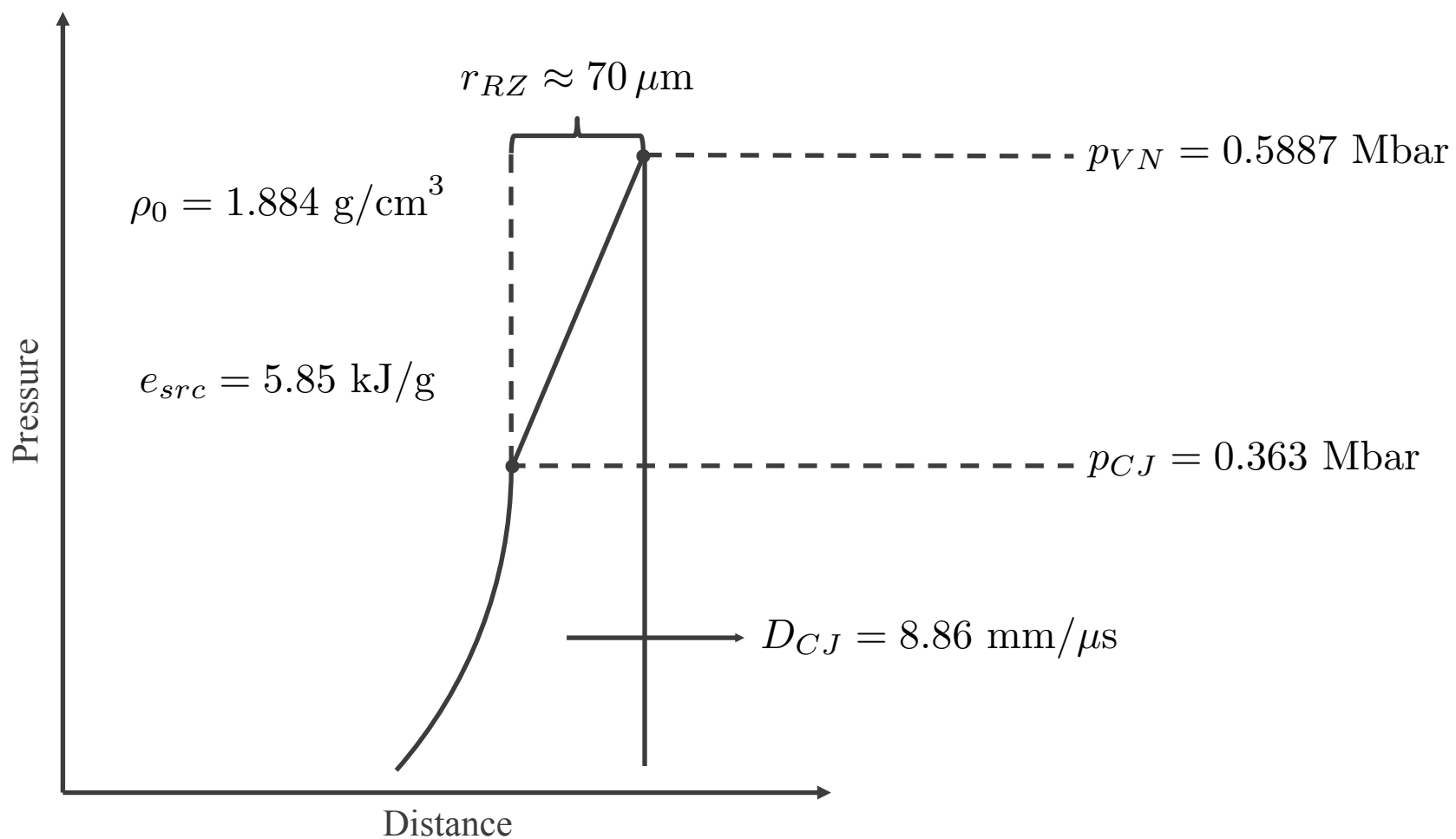


R. Menikoff and M.S. Shaw. Reactive burn models and ignition & growth concept. *EPJ Web of Conferences*, 2010.
R. Menikoff. Shock Detector for SURF model. *Technical Report*, Los Alamos National Laboratory, 2016.

Outline

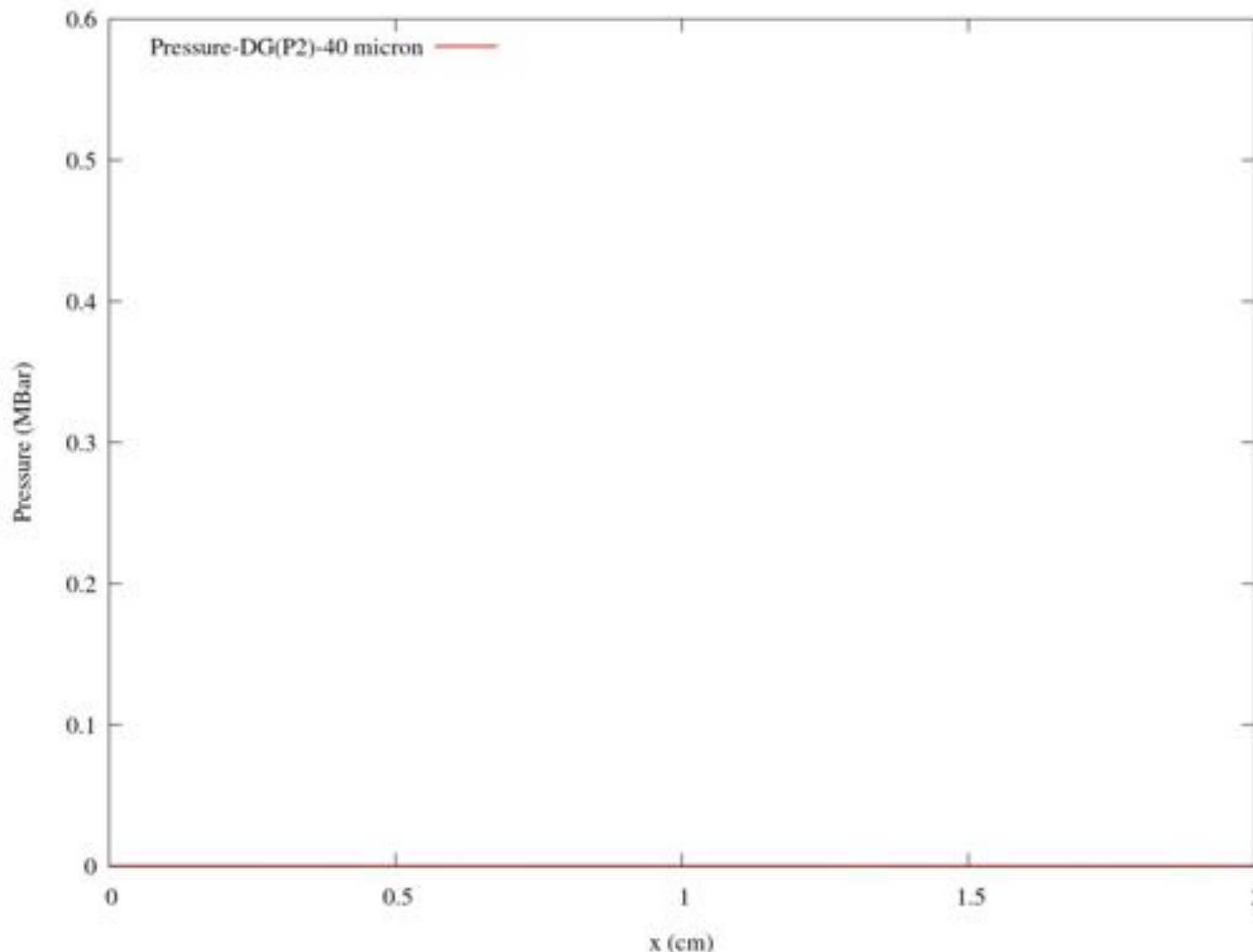
- **Solid Mechanics Models**
 - Deformation Mechanics
 - Constitutive Models
 - Analytic 1D Test Problem
 - 2D Test Problems
 - Summary
- **Reactive Models**
 - ZND Detonation Wave
 - Models
 - Results
 - Summary

Reference Values for ZND Detonation Wave Structure in Shock-to-Detonation Test

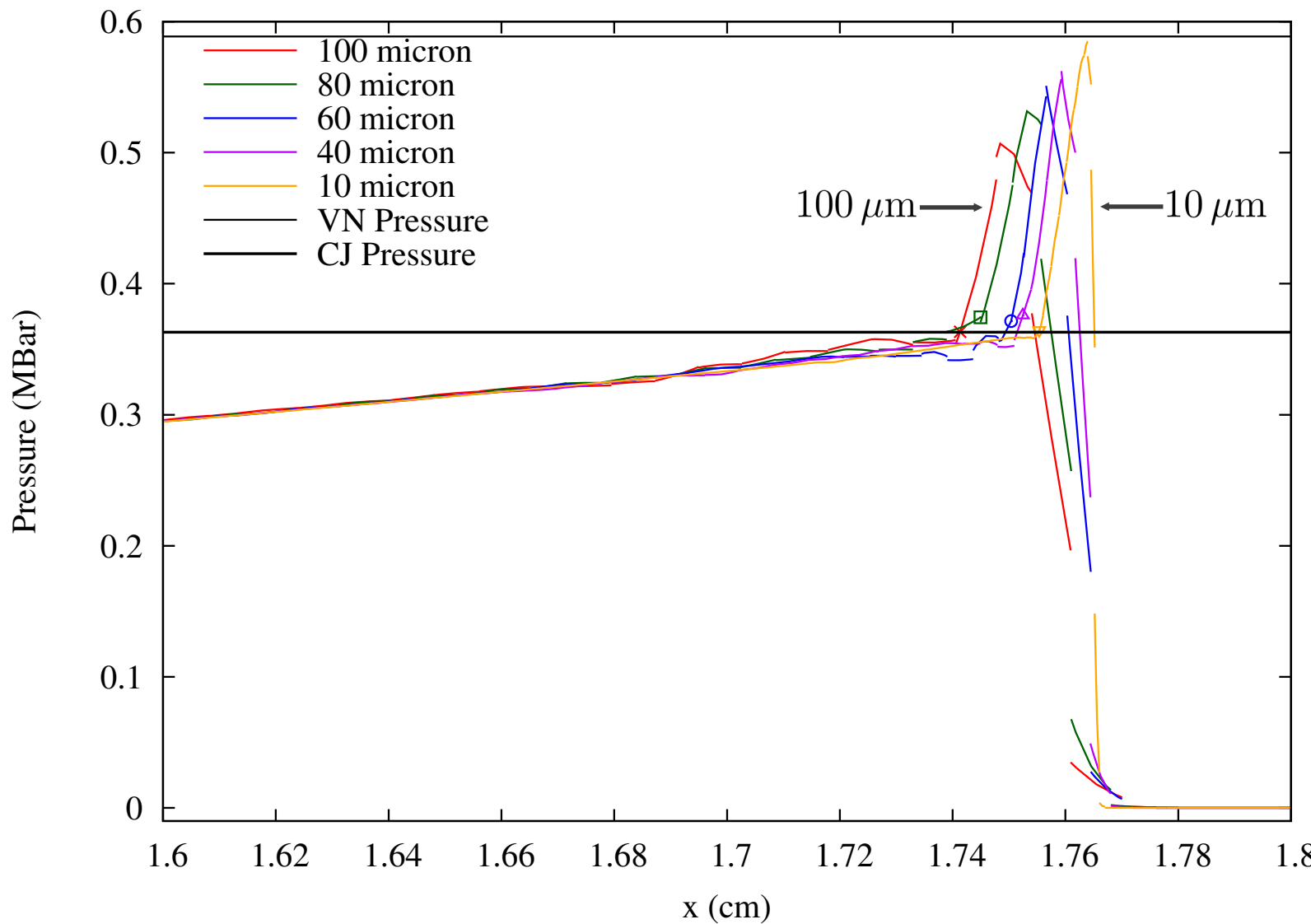


D.E. Lambert, D.S. Stewart, S. Yoo, and B.L. Wescott. Experimental Validation of detonation shock dynamics in condensed explosives. *Journal of Fluid Mechanics*, 2006.

Shock-to-Detonation with SURF using DG(P2) and 40 μm Elements



With Increasing Resolution, Shock Front Sharpens while VN Pressure is More Accurate and CJ is Consistently Accurate



DG(P2) Results are More Accurate than DG(P1)

Correct Detonation Velocity

$$D_{CJ} = 8.86 \text{ mm}/\mu\text{s}$$

Correct von Neumann Pressure

$$p_{VN} = 0.5887 \text{ Mbar}$$

Correct Champan-Jouguet Pressure

$$p_{CJ} = 0.363 \text{ Mbar}$$

Cell Size	Det Velocity ($\frac{\text{mm}}{\mu\text{s}}$)	
	DG(P1)	DG(P2)
100 μm	8.8788	8.8629
80 μm	8.8780	8.8584
60 μm	8.8721	8.8657
40 μm	8.8670	8.8609
10 μm	8.8605	8.8601

Cell Size	VN Pressure (MBar)	
	DG(P1)	DG(P2)
100 μm	0.5441	0.5599
80 μm	0.5517	0.5600
60 μm	0.5594	0.5675
40 μm	0.5678	0.5727
10 μm	0.5847	0.5850

Cell Size	CJ Pressure (MBar)	
	DG(P1)	DG(P2)
100 μm	0.4194	0.3690
80 μm	0.3999	0.3744
60 μm	0.3802	0.3705
40 μm	0.3780	0.3622
10 μm	0.3695	0.3667

At coarse resolutions
the SURF model is
notably more accurate
with DG(P2) than
DG(P1)

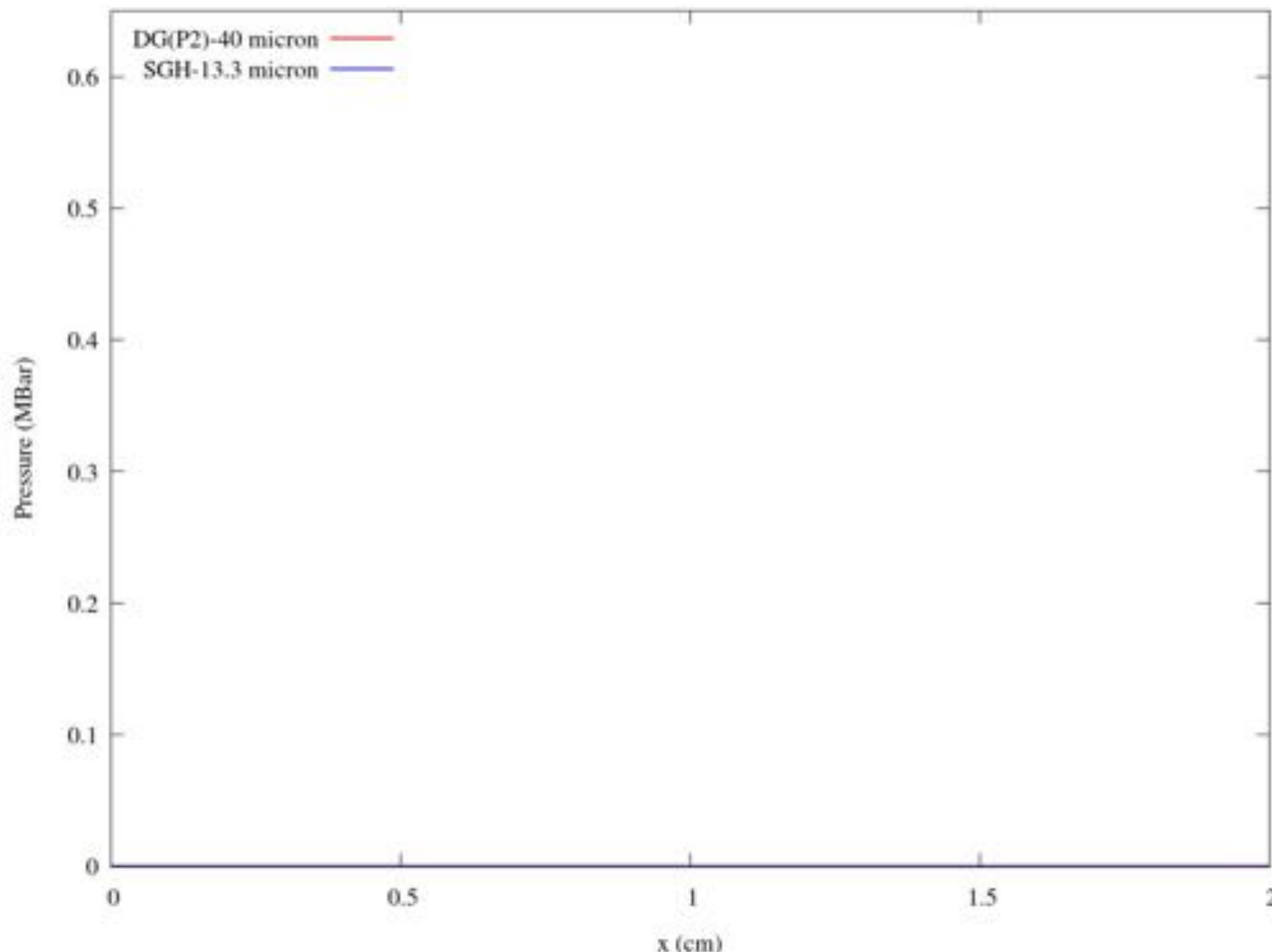
DG(P2) Results are Also More Accurate than Staggered Grid Results for Same Degrees of Freedom

Correct Detonation Velocity

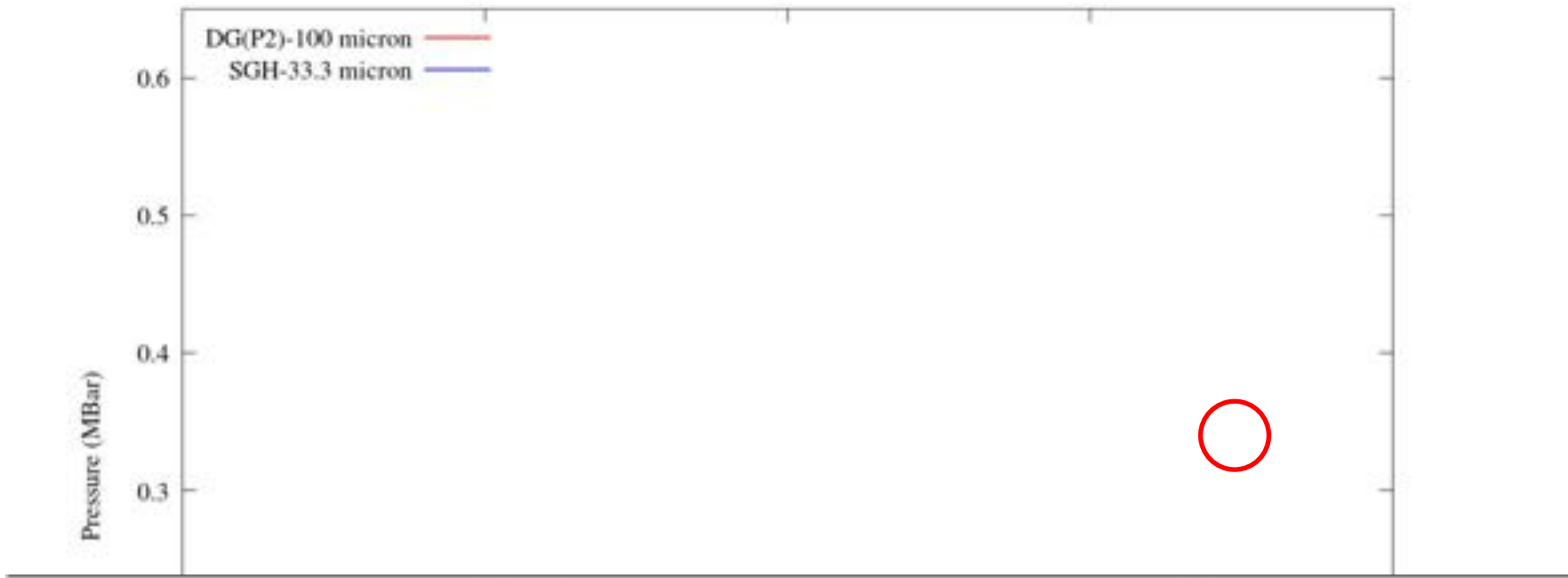
$$D_{CJ} = 8.86 \text{ mm}/\mu\text{s}$$

DoF	DG(P2)		SGH	
	Cell Size (μm)	Det Velocity ($\frac{\text{mm}}{\mu\text{s}}$)	Cell Size (μm)	Det Velocity ($\frac{\text{mm}}{\mu\text{s}}$)
200	-	-	100	9.0477
600	100	8.8629	33.33	8.8948
750	80	8.8584	26.67	8.8790
1000	60	8.8657	20.00	8.8789
1500	40	8.8609	13.33	8.8639
6000	10	8.8601	3.33	8.8609

DG(P2) Results at 40 μm are Commensurate with SGH Results at 13.3 μm



DG(P2) Results are Accurate at 100 μm while SGH at 33.3 has a Fast Det Velocity and Low CJ Pressure



DoF	DG(P2)		SGH	
	Cell Size (μm)	Det Velocity ($\frac{\text{mm}}{\mu\text{s}}$)	Cell Size (μm)	Det Velocity ($\frac{\text{mm}}{\mu\text{s}}$)
200	-	-	100	9.0477
600	100	8.8629	33.33	8.8948
750	80	8.8584	26.67	8.8790
1000	60	8.8657	20.00	8.8789
1500	40	8.8609	13.33	8.8639
6000	10	8.8601	3.33	8.8609

Outline

- **Solid Mechanics Models**
 - Deformation Mechanics
 - Constitutive Models
 - Analytic 1D Test Problem
 - 2D Test Problems
 - Summary
- **Reactive Models**
 - ZND Detonation Wave
 - Models
 - Results
 - Summary

Reactive Materials Summary

- By using a sub-cell method with the programmed burn model, the DG method avoids the problems with overshoots seen with DG and the staggered grid method otherwise.
- The reactive burn model is functional at coarse resolutions using quadratic polynomials with DG, but is not for linear polynomials with DG or with the staggered grid method.
- The results from all methods converge toward the exact solution with resolution refinement.

Future Work for Reactive Materials

- Convergence studies of the method using supported ZND analytic solutions.
- Perform 2D simulations.
- Implement other reactive burn models.

Auxiliary Slides

Hierarchical Limiting of Higher-Order Terms

$$\mathbb{U}(\xi)^{lim} = \bar{\mathbb{U}} + \phi_1 \left(\psi^2 \frac{\partial \mathbb{U}}{\partial \xi} + \phi_2 \psi^3 \frac{\partial^2 \mathbb{U}}{\partial \xi^2} \Big|_z \right)$$

High Order Limiting

$$\frac{\partial \mathbb{U}(\xi)}{\partial \xi} = \frac{\partial \mathbb{U}}{\partial \xi} \Big|_z + (\xi - \xi_z) \frac{\partial^2 \mathbb{U}}{\partial \xi^2} \Big|_z$$

Linear Limiting

$$\mathbb{U}_2(\xi) = \bar{\mathbb{U}} + \psi^2 \frac{\partial \mathbb{U}}{\partial \xi} + \phi_2 \psi^3 \frac{\partial^2 \mathbb{U}}{\partial \xi^2} \Big|_z$$

$$\phi_2 = \begin{cases} \min \left(1, \frac{\left(\frac{\partial \mathbb{U}}{\partial \xi} \Big|_{\xi_j}^{max} - \frac{\partial \mathbb{U}}{\partial \xi} \Big|_z \right)}{\left(\frac{\partial \mathbb{U}}{\partial \xi} \Big|_{\xi_j} - \frac{\partial \mathbb{U}}{\partial \xi} \Big|_z \right)} \right) & if \quad \frac{\partial \mathbb{U}}{\partial \xi} \Big|_{\xi_j} > 0 \\ \min \left(1, \frac{\left(\frac{\partial \mathbb{U}}{\partial \xi} \Big|_{\xi_j}^{min} - \frac{\partial \mathbb{U}}{\partial \xi} \Big|_z \right)}{\left(\frac{\partial \mathbb{U}}{\partial \xi} \Big|_{\xi_j} - \frac{\partial \mathbb{U}}{\partial \xi} \Big|_z \right)} \right) & if \quad \frac{\partial \mathbb{U}}{\partial \xi} \Big|_{\xi_j} < 0 \\ 1 & else \end{cases}$$

$$\phi_1 = \begin{cases} \min \left(1, \frac{\alpha (\bar{\mathbb{U}}^{max} - \bar{\mathbb{U}})}{\mathbb{U}_2(\xi_j) - \bar{\mathbb{U}}} \right) & if \quad \mathbb{U}(\xi_j) > 0 \\ \min \left(1, \frac{\alpha (\bar{\mathbb{U}}^{min} - \bar{\mathbb{U}})}{\mathbb{U}_2(\xi_j) - \bar{\mathbb{U}}} \right) & if \quad \mathbb{U}(\xi_j) < 0 \\ 1 & else \end{cases}$$

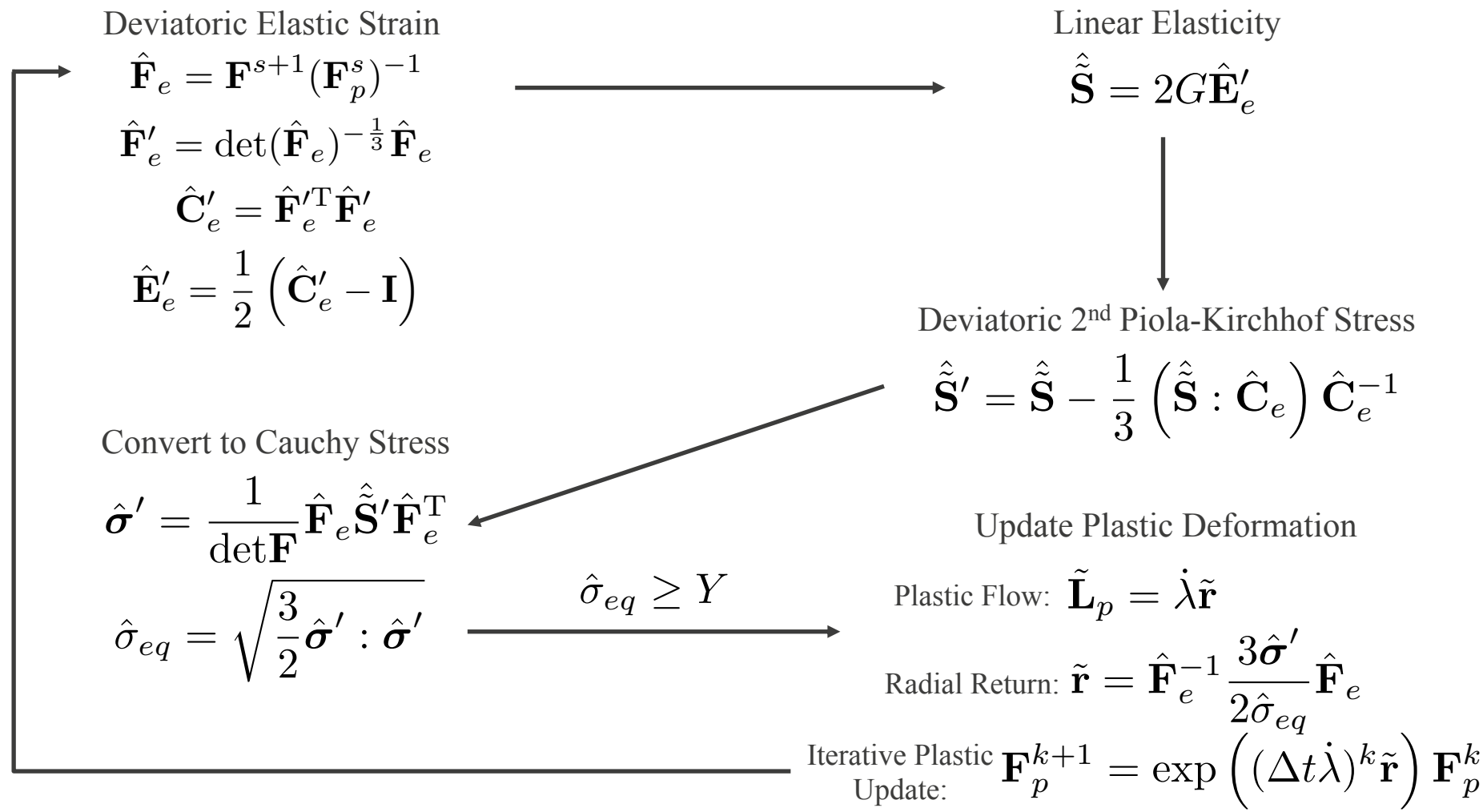
Equation of State Constitutive Model for Solid

$$\boldsymbol{\sigma} = \boldsymbol{\sigma}' - p\mathbf{I}$$

Gruneisen Model

$$\begin{aligned}\eta &= 1 - \rho^0/\rho & \rho^0 &= 2.79 \text{ g/cm}^3 \\ P_H(\eta) &= \frac{\rho^0 c_0^2 \eta}{(1-s\eta)^2} & s &= 1.34 \\ E_H(\eta) &= \frac{\eta P_H}{2\rho^0} & c_0 &= 0.533 \text{ cm}/\mu\text{s} \\ p(\eta, e) &= P_H + \Gamma\rho(e - E_H) & \Gamma &= 2\end{aligned}$$

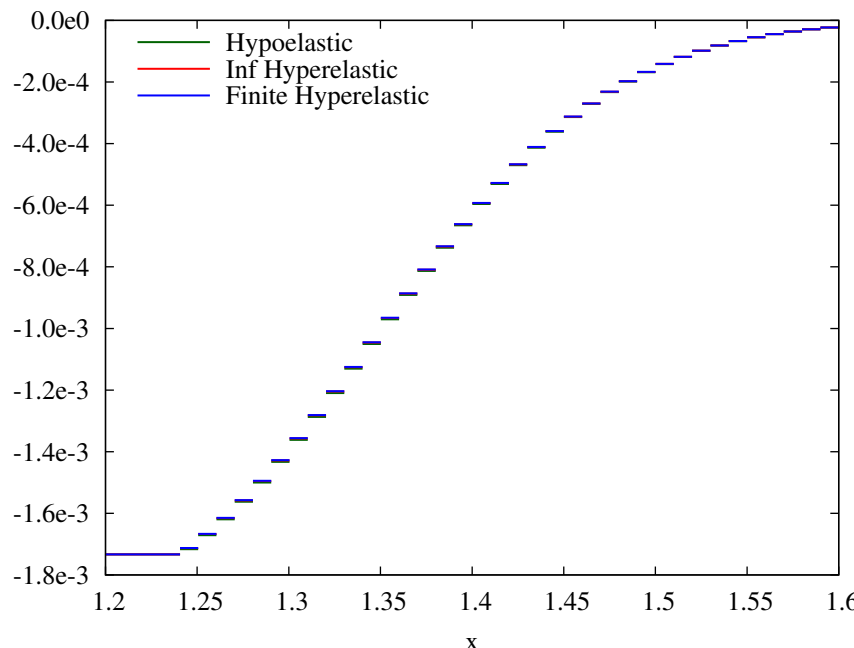
The Finite Hyperelastic-Plastic Constitutive Model



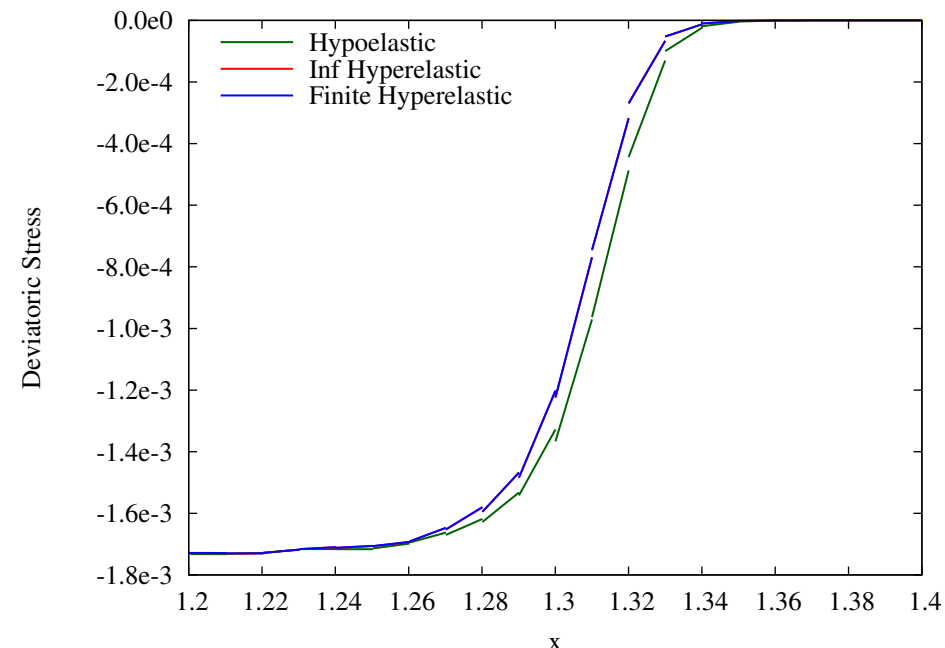
Elastic-plastic Piston Results show large difference between DG(P0) and DG(P1)

Piecewise Constant (P0)

Deviatoric Stress



Linear (P1)

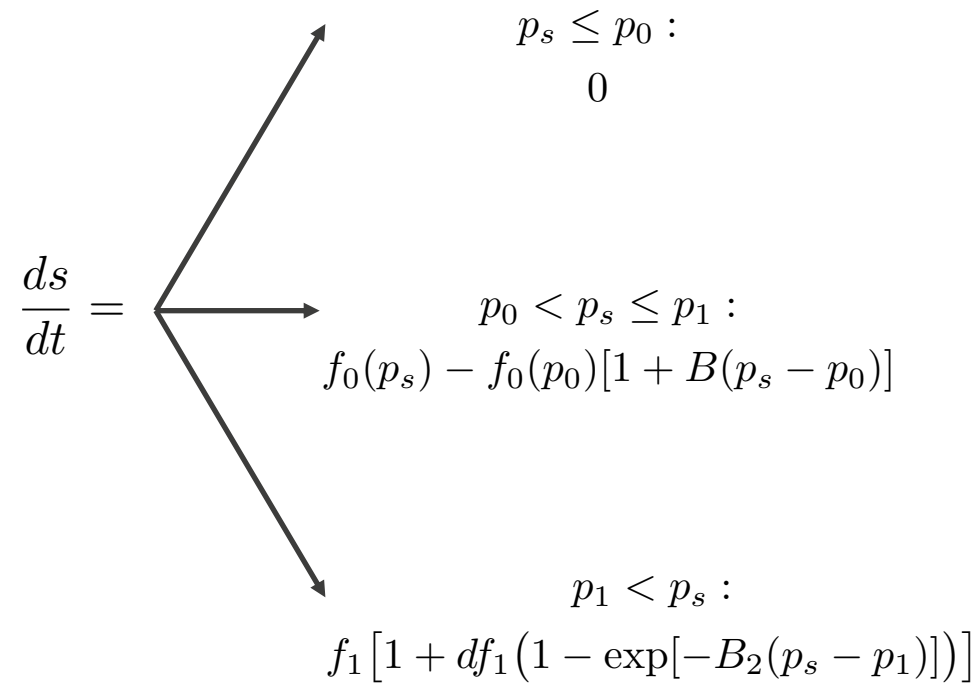


SURF Model Determines Reaction Rate for Different Pressure Regimes

Reaction Rate
as a function of state
 $\lambda = g(s)$

$$\frac{ds}{dt} = f(p_s)$$

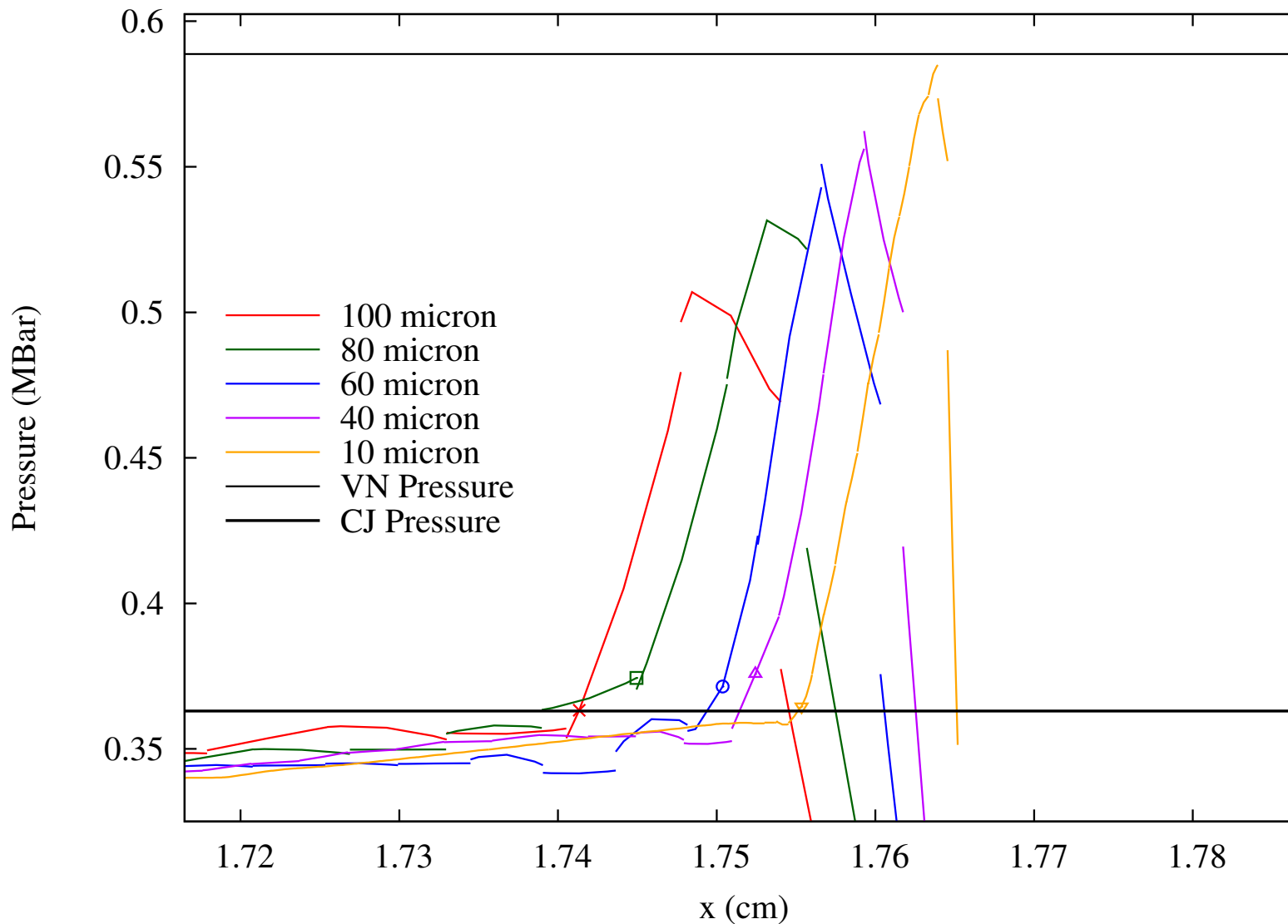
Parameters:
 p_0, p_1, A, B, df_1



$$f_0(p) = \exp(A + Bp) \quad f_1 = f_0(p_1) - f_0(p_0)[1 + B(p_1 - p_0)] \quad B_2 = \frac{B}{df_1} \cdot \frac{f_0(p_1) - f_0(p_0)}{f_1}$$

R. Menikoff and M.S. Shaw. Reactive burn models and ignition & growth concept. *EPJ Web of Conferences*, 2010.
R. Menikoff. Shock Detector for SURF model. *Technical Report*, Los Alamos National Laboratory, 2016.

Shock Front and Reaction Zone are Better Defined with Increasing Resolution



Error Calculation Equations

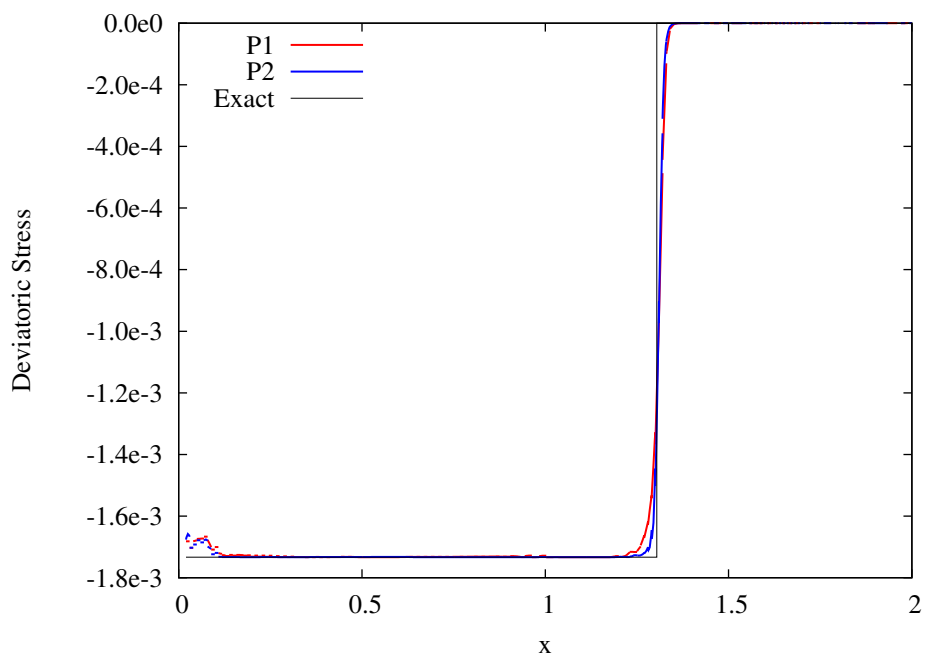
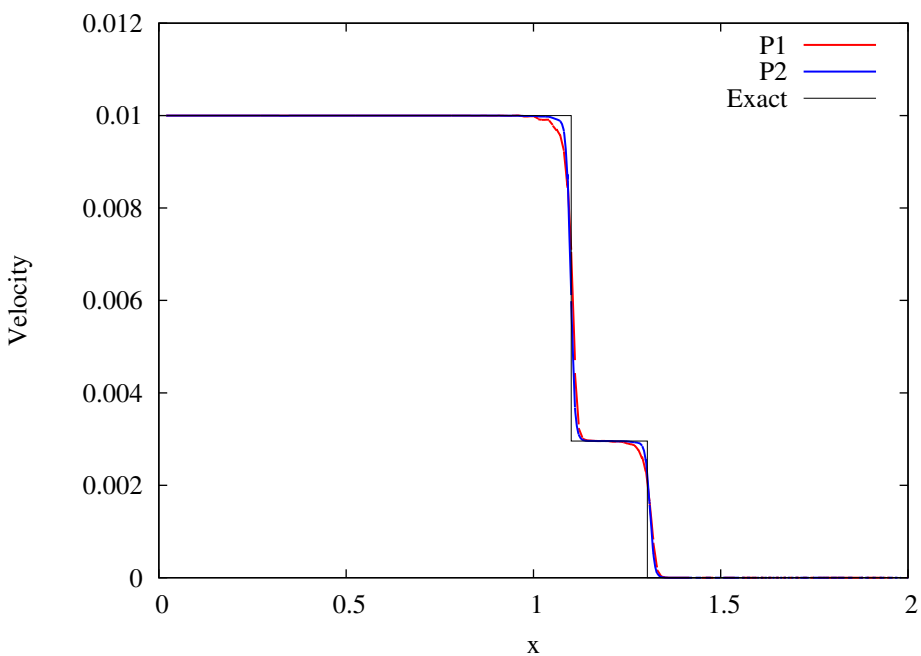
Shock Problems : L_1

$$||\mathbb{U} - \mathbb{U}_a||_{L_1} = \sum_{h=1}^{Num} \int_{\Omega_h} |\mathbb{U} - \mathbb{U}_a| j d\Omega_h$$

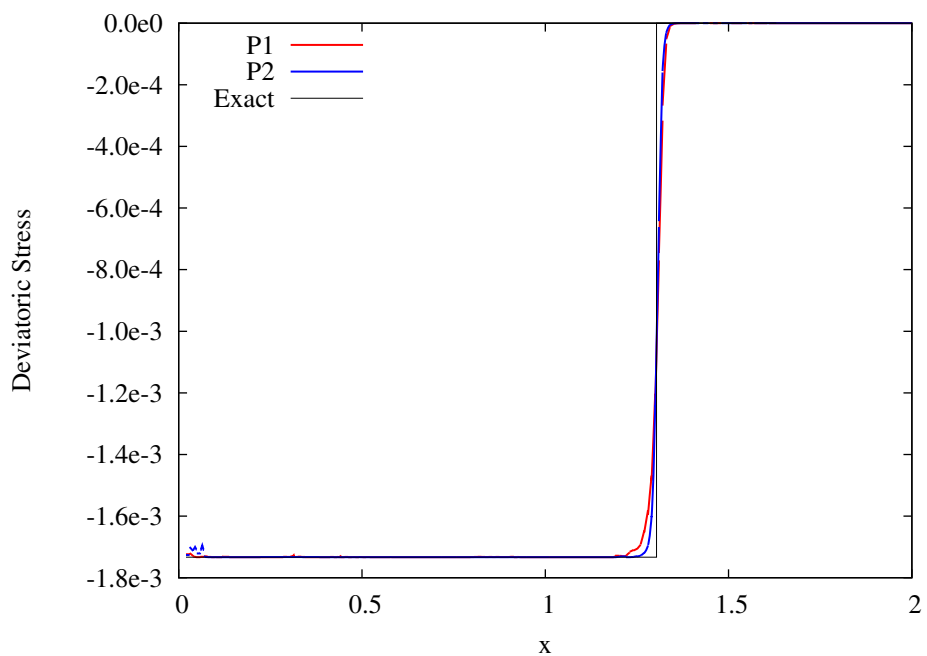
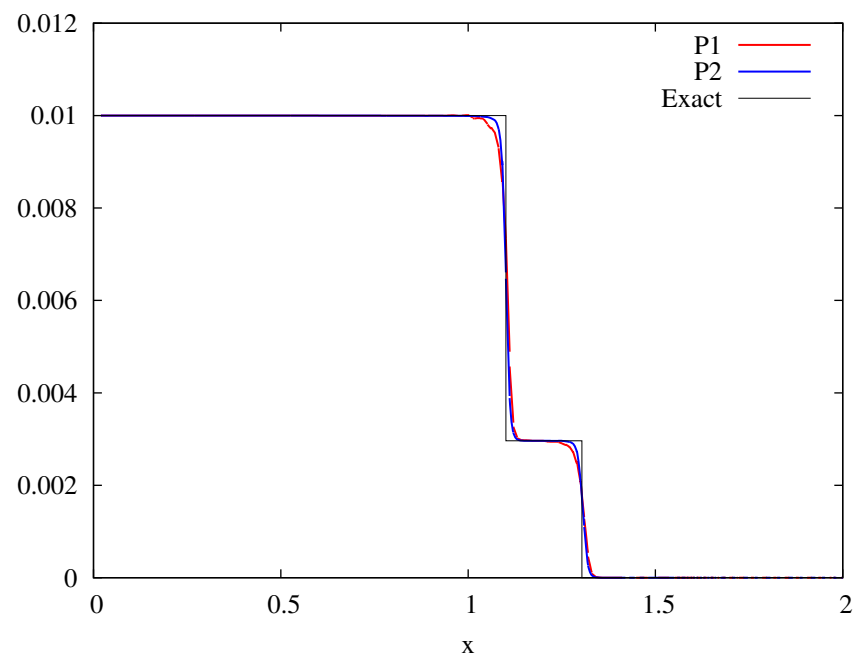
Smooth Flow Problems : L_2

$$||\mathbb{U} - \mathbb{U}_a||_{L_2} = \sqrt{\sum_{h=1}^{Num} \int_{\Omega_h} (\mathbb{U} - \mathbb{U}_a)^2 j d\Omega_h}$$

Elastic-plastic Piston: Hypoelastic Results



Elastic-plastic Piston: Infinitesimal Hyperelastic Results



Elastic-plastic Piston: Finite Hyperelastic Results

